UNIVERSITY OF CALIFORNIA SAN DIEGO

Sensorimotor Processing in Action Timing

A dissertation submitted in partial satisfaction of the requirements for the degree
Doctor of Philosophy

in

Neurosciences

by

Jonathan Ryan Cook

Committee in charge:

Professor Xin Jin, Chair
Professor Willliam Kristan, Co-Chair
Professor Edward Callaway
Professor Martyn Goulding
Professor Christina Gremel
Professor Charles Stevens
Professor Lisa Stowers

2019

The Dissertation of Jonathan Ryan Cook is approved,
and it is acceptable in quality and form for publication on microfilm
and electronically:

_____

_____

_____

_____

_____

_____

Co-Chair

_____

Chair

University of California San Diego

2019

TABLE OF CONTENTS

LIST OF ABBREVIATIONS

4-OHT	4-hydroxytamoxifen
AAV	adeno-associated virus
AuDd	dorsal auditory cortex
AuDp	primary auditory cortex
AuDv	ventral auditory cortex
BET	behavioral theory of timing model
cFOS	immediate early gene protein
ChR2	channelrhodopsin 2
DMS	dorsal medial striatum
ESARE	enhanced synaptic activity responsive element
FosTRAP	mouse for activity-dependent labeling using the cFos promoter
HVC	High vocal center
MSN	medium spiny neuron
Opto-ICSS	optical intracranial self-stimulation
PCC	pearson correlation coefficient
PETH	perievent time histogram
rAAV2	retrograde adeno-associated virus serotype
RPE	reward prediction error
SBF	striatal beat frequency model
SFI	self-paced fixed-interval timing
TRAP	targeted recombination of active populations

LIST OF FIGURES

ACKNOWLEDGMENTS

I would like to acknowledge Ed Callaway, Kuo-Fen Lee, Fred Gage, and Xin Jin for their scientific guidance and mentorship. I would also like to thank Bella Nguyen who played an indispensible role in the generation of the data for my soon to be published work.

I would also like to thank my amazing friends and family who have been a continual source of emotional support during my graduate training, including: Dawn Cook, Nigel Cook, Frances Ford, Candice Lewis, Greg Lewis, Lance Ford, Nancy Ford, Susana Lemons, Brant Lemons, Brittany Lemons, Yousef Rasheed, Catherine McKenzie, Evan Campbell, Josh Baker, Josh Stanley, and DJ Castillo.

Chapters 1-6 and the appendix, in part, are currently in preparation for submission for publication (Jonathan Cook, Bella Nguyen, Payaam Mahdavian, Megan Kirchgessner, Patrick Strassmann, Max Engelhardt, Edward M. Callaway, and Xin Jin). The dissertation author was the primary researcher and author of this material.

VITA

2007-2010	B.S. Biochemistry, University of California San Diego
2010-2012	Research Assistant, Salk Institute for Biological Studies
2012-2019	Doctor of Philosophy in Neurosciences, University of California, San Diego

PUBLICATIONS

Jonathan Cook, Bella Nguyen, Payaam Mahdavian, Megan Kirchgessner, Patrick Strassmann, Max Engelhardt, Edward M. Callaway, and Xin Jin (in preparation). Contribution of adjunctive sensorimotor feedback in self-paced action timing.

Grace Zhu**, Jonathan Cook**, Cheng-Ta Lee, Stephanie Chen and Bertha Dominguez, Kuo-Fen Lee (in preparation). A unique 2:1 imbalance of hyperactivity of the direct and indirect pathways underlies resting tremor and neuropsychiatric disorder.

Maria C. Marchetto, Branka Hrvoj-Mihic, Bilal E. Kerman, Diana X. Yu, Krishna Vadodaria, Inigo Narvaiza, Sara B. Linker, Renata Santos, Ahmet M, Denli, Ana D. Mendes, Ruth Oefner, **Jonathan Cook**, Lauren McHenry, Jaeson Michael Grasmick, Kelly Heard, Callie Fredlender, Rijul Kshirsagar, Rea Xenitopoulos, Alysson R. Muotri, Krishnan Padmanabhan, Katerina Semendeferi and Fred H. Gage (in review). Species-specific maturation profiles of human, chimpanzee and bonobo neural cells. *eLife*.

Huiyun Du, Wei Deng, James B. Aimone, Minyan Ge, Sarah Parylak, Keenan Walch, Wei Zhang, **Jonathan Cook**, Huina Song, Liping Wang, Fred H. Gage, and Yangling Mua (2016). Dopaminergic inputs in the dentate gyrus direct the choice of memory encoding. *PNAS*.

Jiqing Xu, Fred de Winter, Catherine Farrokhi, Edward Rockenstein, Michael Mante, Anthony Adame, **Jonathan Cook**, Xin Jin, Eliezer Masliah and Kuo-Fen Lee (2016). Neuregulin 1 improves cognitive deficits and neuropathology in an Alzheimer's disease model. *Scientific Reports*.

FIELD OF STUDY

Major Field: Neurosciences

Professor Xin Jin, Salk Institute for Biological Studies, San Diego
Professor Kuo Fen Lee, Salk Institute for Biological Studies, San Diego
Professor Fred Gage, Salk Institute for Biological Studies, San Diego

ABSTRACT OF THE DISSERTATION

Sensorimotor Processing in Action Timing

by

Jonathan Ryan Cook

Doctor of Philosophy in Neurosciences

University of California San Diego, 2019

Professor Xin Jin, Chair
Professor William Kristan, Co-Chair

The ability to accurately determine when to perform actions is a fundamental function of the nervous system and vital to shaping behavioral responses that achieve there intended outcome. Fixed-interval reinforcement schedules require animals to respond following a specified interval duration in order to obtain a reward. When reinforcement trials are interleaved with non-rewarded, or probe, trials during training, animals develop peak press distributions in these omission trials around the reinforced time. This peak press distribution under omission conditions indicates animals can correctly start and stop responding in a manner according to when the reward outcome would be expected. The cortex and striatum have been canonically implicated in action timing and behavioral models have proposed the idea that action behavioral states during motor timing performance could play a role in the pacing of action with respect to time. In this dissertation, I describe a sensorimotor feedback mechanism in which modal cortical activation by action-derived sensory cues is utilized to shape response dynamics in a self-paced fixed-interval timing task. Acute deprivation of the action-cued sensory modality, but not other action-based senses, is sufficient to disrupt timing dynamics in trained animals. Staining for immediate early gene protein expression in animals that performed the motor timing task revealed active populations in a modal cortical region related to pressing. Using an activity-dependent labeling system that exploits the *cFos* promoter, action-triggered optical activation of these populations via channelrhodopsin, partially rescues the key features of learned action timing behavior under sensory deprivation. Finally, using a viral activity-dependent labeling strategy in combination with the retrograde adeno-associated virus serotype, I demonstrate a role of layer V, striatal-projecting populations in task performance also under a sensory deprived state. These data point toward a feedback component of motor timing control in which modal cortices and the basal ganglia transduce self-generated sensory cues to assist in performing

complex motor timing patterns.

Chapter 1: Introduction and background

1.1 Overview

Timing is a fundamental dimension of behavior that under many circumstances determines whether an animal's actions achieve their intended outcome. Surprisingly, despite the ubiquity of timing in innate and learned behaviors, our understanding of how the brain calculates time remains relatively unclear. Even in philosophy timing has been a difficult topic to address because of its intangible and subjective nature (1.2.1 Philosophy of timing). An important distinction to make in studying timing behavior is the difference between sensory and motor timing (1.2.2 Motor vs. sensory timing). Sensory timing usually involves subjects perceiving and judging elapsed interval durations defined by stimuli, while motor timing requires subject to produces a precise temporally defined action pattern (Meck and Ivry, 2016; Paton and Buonomano, 2018). Since the performance of sensory timing is implicitly dependent on sensory stimuli, it might not be surprising to learn that altering stimulus features can in turn alter a subject's conception of time (Ahrens and Sahani, 2011; Eagleman, 2008). In contrast, motor timing tasks typically utilize sensory cues to designate only the initiation and/or termination of the interval being learned, leaving subjects to perform timed actions based largely on their own internal representation of time. This has led to idea that motor timing presumably operates on a more self-sustaining mechanism than sensory timing (Meck and Ivry, 2016; Paton and Buonomano, 2018). State based behavioral theories of timing (Killeen and Fetterman, 1988; Machado, 1997) have purported that animals utilize action states to effectively chain together temporally connected patterns of responses (1.2.3 Abstract models for timing). In this view, complex motor timing can be seen as an emergent property of a learned action sequence. Evidence for this has come from the widely observed phenomenon of stereotyped chains of adjunctive behavior that seem to emerge under schedules of temporally defined reinforcement

(Haight and Killeen, 1991; Hodos et al., 2005; Laties et al., 1965; Machado and Keen, 2003; Skinner, 2004). Furthermore, variations of these chains of behavior have been found to correlate to variations in the estimation of interval duration (Gouvêa et al., 2014). One possibility is that action state alone is sufficient to control motor timing, meaning the instructive signal to move provides the necessary information to convey changes in time. However, an intriguing hypothesis is that an understanding of action state is dependent on an implicit sensory awareness of ongoing action. If this were the case, it would be expected that decoupling the sensory modality tuned to action would alter timing performance. State-dependent network models of sensory timing (1.2.4 Neurally inspired models for timing) have described how simple, subsecond-tuned cortical motifs (Buonomano, 2000) can act in concert to allow for interval duration perception of stimuli (Buonomano and Merzenich, 1995; Buonomano and Maass, 2009). These models tell time by relying on the fact that incoming sensory stimuli define a network state that sets the context for how the network will respond to subsequent incoming stimuli. In contrast, population models for motor timing (1.2.4 Neurally inspired models for timing) have described how spatiotemporal firing patterns in recurrent networks can tell time to produce anticipatory actions by behaving in a largely self-sustaining manner, traveling along a specific neural trajectory initiated by limited input to the network (Goldman, 2009; Laje and Buonomano, 2013; Liu and Buonomano, 2009; Miller and Jin, 2013). Physiological evidence of these types of recurrent network patterns in animals performing motor timing tasks (1.2.5 Neurobiological evidence for timing) has been observed in structures like the striatum (Jin et al., 2009; Mello et al., 2015). However, it unclear as to whether these observed population patterns are truly self-sustaining or whether upstream inputs plays a more significant role. Thus, the relationship between adjunctive action patterns and time perception described in state based

behavioral theories (Gouvêa et al., 2014; Killeen and Fetterman, 1988; Machado, 1997) could result from sensory cues related to action state being used to adjust motor responses online, in which case sensory input would play a more significant role in motor timing than previously thought (1.2.6 Hypothesis: action state, sensory feedback and timing).

Using a novel self-paced motor timing task, I explored the role of a self-generated sensory feedback cue in the corticostriatal circuit – a pathway known to be important in the integration of sensory stimuli as it relates to action (Znamenskiy and Zador, 2013). I developed a self-paced fixed-interval timing task (SFI) in which animals have to initiate a fixed-interval and continue responding until the criteria duration has been reached (Chapter 2: A self-paced fixed-interval timing task). The first response at or after the duration criteria has been reached yields a reward. Timing performance in this task is assayed through probe trials in which the reward is omitted. Consistent with other versions of this peak response task, animals develop an adjunctive pressing profile during probe trials with maximal responding around when reward delivery would occur (Gibbon, 1977; Meck, 2006; Roberts, 1981; Ward et al., 2009). Uniquely, animals only have to press twice in the task design, but develop an escalating, repetitive response strategy. In this sense, the additional pressing is considered a collateral or adjunctive action to the response criteria strictly required for obtaining a reward (Falk, 1971). The design of SFI was motivated to eliminate the influence of external cues designating interval initiation and termination so as to maximize the influence of a self-generated sensory feedback cue. An acute sensory deprivation screen demonstrated that animals predominantly relied on hearing to perform the SFI task (Chapter 3: A sensory role in self-paced fixed-interval timing performance). Specifically, the dynamics of responding acquired through learning seemed to be acutely reversed by auditory deprivation and largely returned to original performance levels in post-

deprivation control sessions. Importantly, these deprivation effects were found to be independent of any cues related to reward delivery and cFos staining demonstrated auditory cortex activation, specifically layer V of the dorsal auditory cortex (AuDd), that was dependent on SFI acquisition and lever pressing (Chapter 4: A neural substrate for sensing action in task performance). Pharmacological inactivation of the activated region in the auditory cortex demonstrated the same sensorimotor deficits observed in acute sensory deprivation. Using a transgenic activity-dependent labeling system under control of the *cFos* promoter, targeted recombination of active populations (FosTRAP), I was able to genetically access the active populations in the auditory cortex activated by responding (Guenthner et al., 2013). Activation of these populations in an action dependent manner under sensory deprivation conditions partially rescued the temporal dynamics of action (Chapter 5: Sensorimotor feedback control in task performance). Finally, combining the retrograde adeno-associated virus (Tervo et al., 2016) variant (rAAV2) with a viral-based activity-dependent labeling system (Kawashima et al., 2013), enhanced synaptic activity–responsive element (ESARE), I was able to confirm a contribution of striatal-projecting active populations within the auditory cortex to task performance. The results from my work demonstrate a role for self-derived sensory processing in a motor timing task. The research also places the corticostriatal circuitry as a potential neural mechanism for this type of action self-monitoring in complex motor timing behavior.

1.2 Background

1.2.1 Philosophy of timing

"The idea of time, being derived from the succession of our perceptions of every kind, ideas as well as impressions, and impressions of reflection as well as sensation, will afford us an instance of an abstract idea, which comprehends a still greater variety than that of space, and yet

is represented in the fancy by some particular individual idea of a determinate quantity and quality." David Hume, *A Treatise of Human Nature*, 1740.

The Scottish philosopher David Hume spent a great deal of effort discussing his ideas on time and how we perceive it. Hume was made famous by his deep philosophical skepticism. He believed that many of our intuitions about the world, including morality, were based on a flawed understanding of causality. For Hume, just because one event preceded another does not necessarily mean the two events were related. He felt that humans had a tendency to over emphasize prior information. Since one would always have to extrapolate from the past, establishing explicit causality was hard if not impossible. Hume admitted of course that this mindset was not the most practical method for going about one's life, but his skepticism laid an important foundation for understanding basic psychological processes, i.e. our intuition of how our brains goes about performing everyday functions may not necessarily match reality. Rather than seeing our sense of time as a "determinate quantity", Hume saw it as highly malleable, dependent on sensory perceptions and more an emergent property of experience than a discreet brain function. Earlier philosophers like Aristotle also echoed this skepticism about discussing time perception. When asked "What is time?", Aristotle factiously responded "What is a ghost?". The philosopher J.M.E. Taggart took this skepticism even further, by providing a simple thought experiment. If all organisms in the world died, could physical events, such as a volcano erupting, be said to be in the future? Without a conscious observer how is a reference established upon which time can be established? These skeptical viewpoints ironically produced an important starting point for timing psychology, which is the fact that our sense of time is deeply related to our conscious sensory awareness of what is going on around us.

Examples of the impact of sensory experience on time perception are abundant. For instance, changing the flicker rate of visual stimuli is known to cause a dilating effect on the perception of time, such that stimuli that flicker at a higher rate are perceived to last longer (Ahrens and Sahani, 2011). Furthermore, moments of terror, in which sensory load and saliency are heightened, are perceived as occurring slower (Stetson et al., 2007). In addition, if a subject is shown repeated presentations of an object for a set duration of time and a random object is then introduced for the same duration, the "oddball" object is perceived to last longer (Eagleman, 2008). This theme of conscious sensory perception and its effect on time also applies to large-scale durations, such as years. Childhood years are commonly remarked to seem longer than adult years. This effect is believed to be associated with the accumulation of a large amount of novel, sensory rich experiences in childhood. As the novelty of everyday life wanes with age, our sense of time speeds up, causing mature years to appear perceptually accelerated relative to our younger ones. An important distinction to make when discussing sensory stimuli in the context of timing is the nature of its source. Most sensory stimuli discussed in timing literature refer to external cues (i.e. stimuli put upon the subject). However, under situations where timing is internally driven (i.e. where an individual has to produce a timed action pattern), sensory cues can be self-generated, much like a piano player hearing the sound generated from pressing a key. Uniquely, my research on the role of sensory stimuli and its effect on timing has attempted to demonstrate how these types of self-generated cues are fed back to alter timed motor responses.

1.2.2 Motor vs. sensory timing

As previously mentioned, timing behavior can be loosely divided into two overarching categories: motor and sensory timing. In a sensory timing task, subjects use action only to express their understanding of experimentally defined stimuli duration (Meck and Ivry, 2016;

Paton and Buonomano, 2018). In this sense, the action required to perform a sensory timing task does not play a direct role in timing per se. In contrast, motor timing actually requires the performance of actions that vary with respect to time (Meck and Ivry, 2016; Paton and Buonomano, 2018). Thus, while sensory timing is dependent on stimuli put upon the subject, motor timing requires the subject to independently generate timed actions. As such, we can think of sensory timing as a more passive form of time-dependent behavior. Since motor timing requires a continual updating of time to guide actions online and occurs in the absence of temporally defined stimuli, the neural mechanism for this type of behavior is believed to be more internally driven. However, these two types of timing actually exist at opposite ends of a spectrum. While a task may be mostly sensory or motor by design, it can never be said to be exclusively one or the other.

A classic example of a sensory timing task is the interval discrimination paradigm (Paton and Buonomano, 2018; Soares et al., 2016). In this task, subjects are trained to discriminate between a long and short duration. Visual or sound cues are played and two levers are presented. For instance, 2 s of sound may be used to condition a left lever response, while 6 s may be used to condition a right lever response. Incorrect responses result in no reward, or a time out from task engagement. Following training, animals will receive a reward on most trials, indicating they can correctly discriminate between the long and short duration. Once an animal is fully trained, the experimenter can then test intermediate stimuli durations during a probe session. For instance, in the case of the 2 s versus 6 s task design, they might present 3 s, 4 s or 5 s durations for a probe session. From this data a psychometric curve can be constructed showing the percent likelihood that the subject will choose the short or long lever for these intermediate durations. Compiling data from these probe session revels that a subject will perform roughly at

chance (50 %) for the bisection of the two conditioned times (i.e. 4s for the example times given) and will press the longer conditioned lever above chance for durations larger than the bisection.

Motor responses in the interval discrimination paradigm serve only to express the subject's judgment about the length of time a stimulus is presented. However, observations of animals performing this task have revealed some interesting unintended, or adjunctive, behaviors that emerge during stimulus presentation prior to action selection (Gouvêa et al., 2014). Adjunctive, or collateral, behaviors are idiosyncratic actions that are not explicitly required for the performance of a task, but emerge with training (Falk, 1971). While some behaviorist have said these actions play no adaptive role in task performance, abstract models of timing have hypothesized how these adjunctive action patterns may actually serve to assist animals in performing time-dependent behavior (Killeen and Fetterman, 1988; Machado, 1997). In the interval discrimination task, the most common adjunctive behavior observed involves animals pacing between the short and long lever during stimulus presentation (Gouvêa et al., 2014; Machado and Keen, 2003). Interestingly, experiments have been performed tracking these action pattern and have demonstrated that trial-by-trial variations in movement do indeed correlate with an individual animal's subjective conception time, based on probe session data where they are exposed to intermediate stimuli durations (Gouvêa et al., 2014). Thus, the interval discrimination task, which is traditionally considered to be a sensory timing behavior, appears to have a motor timing performance component.

A classic example of a motor timing task is the fixed-interval, peak timing task (Gibbon, 1977; Meck, 2006; Roberts, 1981). My research has utilized a variation of this task to study motor timing. Fixed-interval tasks reward animals following a response that occurs at or after an experimentally imposed delay. With training animals develop a scalloping response

profile in anticipation of the time that the reward is available. Probe trials can be introduced to test how animals perform in the absence of rewards. In probe trials, animals typically escalate responding prior to the time of reward delivery and deescalate responding upon realization that the reward will not be delivered. Thus, under reward omission conditions animals form a peak press distribution around the conditioned reward time. Since animals have to generate an action pattern independent of temporally defined sensory cues, this behavior is considered to be purely motor in nature. In some studies, sensory cues are utilized in the task design to indicate when the clock is initiated, or when the reward is available following a response (Gibbon, 1977; Meck, 2006; Roberts, 1981). While these sensory cues do not vary with respect to time, and thus cannot provide the animal with any information about time, they are integrated into the task design to assist the animal in learning when to start and stop responding during reinforcement trials. In designing a motor timing task, I sought to diminish the experimentally imposed sensory features of the fixed-interval peak timing task design to the greatest extent possible by making the initiation and termination of the fixed-interval dependent on the animal's own actions. I found that under this task design, sensory information still plays a significant role in motor timing performance. However, in the absence of experimentally imposed sensory cues, animals appear to rely on sensory cues from their own actions. In the same way that action patterns seem to be utilized to inform temporal state in the interval discrimination task, these self-generated sensory cues appear to assist animals in controlling the temporal dynamics of their motor responses.

1.2.3 Abstract models for timing

Several abstract models of timing have been described based largely on behavioral data. While there have been numerous abstract models proposed to explain timing, for the purposes of this introduction I will discuss two of the most influential in the field: the scalar theory of timing

and the behavioral theory of timing. The scalar theory of timing was one of the earliest theoretical explanations of timing and was based on a hypothetical clock system, grounded in experimentally observed behavioral data (Gibbon, 1977). In this model, the clock is composed of a pacemaker and accumulator. The accumulator resets to zero at the beginning of a trial. Once a trial begins, the accumulator receives pulses from the pacemaker. The amount of pulses received by the accumulator is continually compared to a reference memory that dictates via working memory if a response should or should not be made at a particular time. The name of this theory comes from the scalar property of timing. This property is similar to Weber's law and describes how the variability of timed behavioral responses changes proportionally with the experimentally imposed duration. For instance, in the fixed-interval peak timing task discussed above, the experimenter can choose to reward the animal at 10s, 20s or 30s for instance. Using one of these reinforcement times, animals will develop peak press distributions in probe trials. The center of these distributions will always be around the experimentally selected reinforcement time, however, it has been observed that larger selected durations will yield wider peak response distributions. In other words, small rewarded intervals (e.g. 10s) will yield narrow response distributions, while larger rewarded intervals, such as 30s, will yield broad response distributions. While the scalar theory of timing has been extremely influential in explaining timing behavior, it has not translated very well at a neurobiological level. No evidence of a brain structures corresponding to an accumulator or pacemaker have emerged.

Perhaps the other most influential abstract theory of time perception is the behavioral theory of timing (BET). This theory was based on the observation that animals engage in repetitive, ritualistic-like action patterns when trained on temporal reinforcement schedules (Killeen and Fetterman, 1988). According to this theory: "When a reinforcer occurs, for, say,

pecking a key, the animal associates the current behavioral class with pecking. According to BET, the behavioral class serves as discriminative stimuli or cues that set the occasion for the operant response" (Machado, 1997). The collateral action patterns that emerge under temporal reinforcement are called adjunctive behaviors because they are not strictly required for the animal to perform the task, but appear as an unintended consequence of the reinforcement schedule. In the interval discrimination paradigm, as previously stated, animals pass between the short and long lever during stimulus presentation and these action patterns seem to be related to animals' subjective conception of time (Gouvêa et al., 2014). In the peak interval procedure, animals have to press the lever to obtain a reward following a fixed-interval of time. Animals only have to press to obtain the reward, but ultimately engage in a repetitive pressing strategy. In this sense, the additional pressing can be described as adjunctive, as it is not explicitly required for the animal to perform the task. Some versions of the fixed-interval peak task initiate the clock with an externally imposed cue and then have the animal press to obtain a reward. In these task designs, animals tend to engage in pressing bouts only around the reinforced time during probe trials, rather than continuously pressing the lever. Consequently in these task designs, animals can engage in other idiosyncratic temporal mediating behaviors like twirling in place or tail biting (Laties et al., 1965). In designing a fixed-interval peak timing task, I sought to control adjunctive behaviors as much as possible. I achieved this by making the fixed-interval task self-initiated, rather than using an external cue to signal clock initiation. By making the fixed-interval self-initiated (i.e. animals have to press the lever once to start the clock) animals resorted to continuously engaging with the lever post initiation press. This design feature served as an important starting point for studying the role of adjunctive behavior in timing, as it suppressed the development of other collateral behaviors that could not be tracked.

1.2.4 Neurally inspired models for timing

Several neurally inspired models have been proposed to explain timing behavior. Here I will discuss four of these models: the striatal beat frequency model (SBF), ramping models, state-dependent models, and population models. The SBF model was an early attempt to provide a neurobiological substrate for the clock and accumulator described in the scalar theory of timing and could be applied to both sensory and motor timing behavior (Matell and Meck, 2004; Meck et al., 2008). According SBF, cortical neurons oscillate at different frequencies (e.g. 5-15Hz). Individually, these frequencies are incapable of discriminating large scale durations, however, by looking at the coincident interaction of their firing patterns, or beat frequency, it would be possible in theory to encode longer durations. Anatomically, cortical neurons send dense projections to the striatum from layer V. Individually, medium spiny neurons in the striatum receive inputs from multiple cortical neurons, thus making them good candidates for coincidence detection in the brain (Matell and Meck, 2004). The authors describing SBF thus proposed that medium spiny neurons served as "accumulators" in the scalar theory of timing detecting the coincident firing patterns of upstream cortical "pacemaker" neurons. Unfortunately, little neurobiological evidence of this theory has emerged, however, it served as important starting point for describing how the physiological and anatomical properties of the brain might encode time.

Ramping models of timing are based largely on recording data from animals performing motor timing tasks, such as the fixed-interval peak timing task. Neurons in the cortex and basal ganglia have been found to gradually increase or decrease their firing rates across the learned interval duration (Matell et al., 2003; Mita et al., 2009; Murakami et al., 2014). In ramping models, it is proposed that time is encoded through this steady change in

firing rate. A large confound of this model is the fact that animals are often engaging in escalating motor behaviors during the timed interval. As such, divorcing these neural signatures from motor performance is challenging. Some evidence of this model has come from dual peak timing tasks in which animals are taught to peak at two separate times (Matell et al., 2003). Recordings in the striatum have revealed populations of neurons that ramp at one reinforced time and not the other, pointing to the possibility that the encoding of time via ramping is mutually exclusive from the encoding of action.

State-dependent models of timing have attempted to specifically explain sensory timing behavior. According to this group of models, neurons are activated by incoming sensory stimuli, which initiate state changes in the network (Buonomano and Merzenich, 1995; Buonomano and Maass, 2009). As a result of these state changes, the network of neurons will respond differently to early stimuli versus later stimuli allowing for the encoding of elapsed time. The network is setup to change across states as a result of short-term plasticity acquired through learning. There has been some evidence to support this theory in the auditory system. In one study, rats were trained to recognize a two-element sound sequence, with a pause in between the two sounds. Following training, recordings in the auditory cortex revealed that the first sound caused an expansion of response properties, whereby neurons seemed to anticipate and respond more strongly to the subsequent incoming stimuli (Zhou et al., 2010). It is important to note that state-dependent models are inherently passive, meaning that they rely on incoming sensory stimuli to drive the state changes that can tell time. As such, they cannot explain motor timing, where action patterns are independently generated without temporally varying stimuli.

Population models of timing attempt to explain motor timing behavior and as such

are capable of operating in a more autonomous manner. These models describe recurrent network patterns that appear with the learning of timed motor responses. The central idea of these neurally inspired models is that firing patterns propagate through a chain-like network (Goldman, 2009; Laje and Buonomano, 2013; Liu and Buonomano, 2009; Miller and Jin, 2013). This model is based on the observation of reproducible spatiotemporal patterns that emerge in motor structures following time-dependent motor training (Mello et al., 2015; Peters et al., 2014). In contrast with state-dependent models that require continual sensory input, population models are self-sustaining firing patterns that are presumed to operate independent of upstream inputs following training. Interestingly, however, a new model has been proposed showing that population networks in the striatum, for instance, might be molded by cortical projections during training (Murray and Escola, 2017). In this way, the cortex is thought to "tutor," or mold these autonomous neural trajectories that appear later in training. This is based on the experimental data that has shown that motor cortex is necessary for the acquisition of timed motor sequences, but redundant once the behavior is fully acquired (Kawai et al., 2015).

My research on self-initiated, fixed-interval peak timing shows a sensory feature in a motor timing task. As described, population models operate in a self-sustaining manner, while state-dependent models are passive and require continual sensory input. One possibility is that under a task design in which animals have to track their action patterns to correctly time responses, components of both models become necessary for task performance. Sensory input from the animal's own actions may play a role in sustaining the internally generated neural trajectories necessary for timed motor responses. My research has implicated both a sensory cortical region and its striatal projections as necessary neural components for task

performance even once animals are fully trained on a motor timing task, pointing to the possibility that motor timing and sensory timing models could act in concert.

1.2.5 Neurobiological evidence for timing

A large amount of the evidence for timing in the brain to date has been correlative and based on the appearance of time related neural activity (Matell et al., 2003; Mello et al., 2015; Mita et al., 2009; Murakami et al., 2014; Peters et al., 2014). However, with the advent of optogenetics, researchers are beginning to causally test the role of certain brain structures that might be involved in timing. Dopamine has long been hypothesized to play a role in timing because of how reward is known to modulate temporal experience (Malapani et al., 1998; Meck, 2006). Reward prediction error (RPE) describes the activity pattern of dopamine neurons to changes in cued reward outcomes and has been cited as a key piece of experimental evidence for timing in the brain (Schultz et al., 1997). Dopamine neurons respond to the presence of a reward by increasing their firing rate. However, if a cue is repeatedly presented at a set amount of time prior to reward delivery, dopamine neuron responding slowly attenuates. If, however, the reward is omitted following cue-reward conditioning, a dip in dopamine responding is observed at the time the reward would have been delivered relative to the cue. This finding indicates that dopamine neurons are capable of encoding the learned duration between the cue and reward. This finding led researchers to believe that modulating dopamine neurons firing patterns might change an animal's temporal expectation.

In a recent study using a version of interval discrimination task, researchers used fiber photometry to study the firing patterns of nigral dopamine neurons using the genetically encoded calcium indicator, GCamp (Soares et al., 2016). In the task used for this study, animals hear two successive tones separated by varying durations and make a short or long judgment

relative to 1.5s. The authors recorded the magnitude of nigral dopamine responses at the choice event for each interstimulus duration and divided these into a high, medium and low tercile. Each magnitude tercile was plotted as a psychometric curve based on the probability of a long choice versus the actual interstimulus time. If dopamine changes reflected movement, their response magnitude would change choice probability in the same way across all interstimulus durations, resulting in a y-shift between the three curves. However, if changes reflected a time-dependent component of the decision, the terciles would shift horizontally, meaning that dopamine response for a short choice differs than for a long choice. Ultimately, the authors demonstrated an x-shift. They went on to use optogenetic techniques to activate/inhibit dopamine neurons demonstrating the same psychometric x-shift, thus causally linking nigral neuron firing to the control of temporal judgment.

Similar RPE-like patterns have also been observed in the visual cortex of animals performing timing tasks. For instance, studies in the visual cortex have revealed that the presentation of a brief visual stimulus preceding a reward through training can lead to the embodiment of cortical activity occurring at the reward target interval time, which may drive timed motor responses (Namboodiri et al., 2015; Shuler and Bear, 2006). As previously discussed, other correlative evidence of ramping patterns and reproducible spatiotemporal firing patterns in motor structures have also been observed in the brain while animals are performing motor timing tasks (Matell et al., 2003; Mello et al., 2015; Mita et al., 2009; Murakami et al., 2014; Peters et al., 2014). However, testing the role of these physiological features of timing is difficult, since reproducing these precise patterns is not possible. In working on causally testing factors that affect timing in SFI, I sought to manipulate an unconventional aspect of a motor timing task – sensory processing. Rather than directly manipulating motor performance, I

chose to look at the impact of sensory feedback on the motor response. This approach was advantageous as manipulation of motor structures in motor timing tasks always runs the risk of obtaining a result that is an artifact of motor change rather than a manipulation of timing.

1.2.6 Hypothesis: action state, sensory feedback and timing

In reading the literature on timing behavior, I wanted to create a hypothesis that synthesized several of the key findings in the field, while also creating a unique starting point for discovery. These findings included: (1) sensory change modulates sensory timing, (2) adjunctive action patterns inform motor timing, (2) motor timing is an active/internal process and (3) sensory timing is a passive/external process. As I have previously discussed, in the interval discrimination paradigm, animals' action patterns have been found to assist performance, indicating motor timing could play a role in influencing sensory timing performance (Gouvêa et al., 2014). For my thesis work, I wanted to address the reverse of this finding: what sensory aspects of a motor timing task influence performance? However, in the probe trials of my self-initiated fixed-interval peak task, it is hard to think of what sensory features might influence performance, since these trials simply provide the animal with a lever and no external sensory cues are given to the animal. Under this situation it would seem logical to assume that sensory features are almost completely absent and that performance is sensory independent. However, what if sensory cues could come from animals' own actions? In other words, could sensory feedback be utilized to inform motor timing performance, and if so, how are these self-generated sensory cues processed by the nervous system to inform timing? I hypothesized that animals may integrate sensory cues derived from their own actions as a means of updating motor timing behavior and that sensory structures in the brain might mediate this action self-monitoring process.

Parts of this introduction are currently in preparation for submission for publication (Jonathan Cook, Bella Nguyen, Payaam Mahdavian, Megan Kirchgessner, Patrick Strassmann, Max Engelhardt, Edward M. Callaway, and Xin Jin). The dissertation author was the primary researcher and author of this material.

Chapter 2: A self-paced fixed-interval timing task

2.1 Task design

Animals were trained under a novel, self-paced fixed-interval reinforcement schedule (SFI) to yield robust response patterns that varied with respect to time. Fixed-interval operant schedules typically involve cues signaling either the initiation or termination of the designated fixed-interval to encourage acquisition of the time-dependent schedule (Meck, 2006; Roberts, 1981; Wiener et al., 2008). In an effort to force animals to rely predominantly on intrinsic timing mechanisms, rather than external cues, both the initiation and termination of the fixed-interval were made action-dependent (Figure 1A). With training animals developed robust, peak press distributions around the reinforced interval during reward omission, or probe, trials providing an objective readout of the animal's temporal control of action.

In brief, animals were placed in a modular operant chamber and trained to press a lever to receive a reward pellet (Figure 1B). A single lever press initiated the fixed-interval timer and the first press on or after the specified duration (30s) yielded a reward for 70% of the trials. Omission, or probe, trials were randomly interleaved between rewarded trials to assay the animal's response pattern in the absence of reward delivery. Furthermore, for both reward and omission trials, the lever remained out a total of 100 s post lever press initiation, making the two trial types indistinguishable in terms of the duration over which the lever was available for responding (Figure 1A). Lever extension and retraction served only to demarcate trial progression and provided no information on the initiation or termination of the fixed-interval duration itself.

2.2 Learning

Early in training, animals distributed lever pressing evenly across the 100s omission trial

windows. Later stages of training, however, were characterized by dynamic patterns of responding reflecting fixed-interval learning (Figure 1C). To quantify the learning I calculated the response rate at 30s from the perievent time histogram (PETH) of the response raster (Figure 1C, day 21: middle). As training proceeded, animals increased responding around the reinforced time during omission trials, resulting in the formation of a peak press distribution at 30s (Figure 1E: one-way ANOVA, $F_{(4,36)} = 19.10$, $p < 0.0001$, Tukey's multiple comparison test, day 1 vs. day 21, $p < 0.0001$). Normalizing the response rate PETH to the maximum response rate revealed aspects of learning dynamics not immediately obvious (Figure 1C-D, bottom). Most notably, learning is characterized by subtle changes from 0 to 30s, and dramatic reductions in relative responding occurring after 30s. Thus, as a metric of overall response dynamics, or timing, I calculated the half peak fall time (Figure 1C, day 21: bottom), or the time elapsed to reach half the maximum response rate during response de-escalation. This metric had a large dynamic range and decreased across learning as the peak distribution narrowed (Figure 1F: one-way ANOVA, $F_{(4,36)} = 47.05$, $p < 0.0001$, Tukey's multiple comparison test, day 1 vs. day 21, $p < 0.0001$). In contrast to the half peak fall time, the peak time (Figure 1C, day 21: bottom) changed only marginally with learning (Figure 1F: one-way ANOVA, $F_{(4,36)} = 5.870$, $p = 0.0010$, Tukey's multiple comparison test, day 1 vs. day 21, $p = 0.0056$). The half peak fall time thus served as a more accurate indicator for capturing overall changes in timing dynamics.

2.3 Correlated rise and fall response rate changes across learning

To form peak dynamics animals specifically adjust response rates differentially over the course of the 100s omission trials. One possibility is that these time dependent changes in action state are acquired independently of one another. However, another possibility is that these transitions are mutually dependent. Behavioral models of timing have proposed that sequences

of behavioral action states might play a role in the pacing of action with respect to time (Killeen and Fetterman, 1988; Machado, 1997). Under conditions in which few to no external cues can be used to gauge time, such as under the SFI schedule, a strategy such as this would be especially suitable. If this were the case, response rates at one point in time should have a bearing on overall timing dynamics through their effects on response rates at other time points.

I asked how changes in response rates at 30s across learning relate to concurrent changes in response rates at other time points for omission trials. Based on the learning PETHs, increased responding at 30s (Figure 1D, top), seems to occur in parallel with large relative decreases in responding at later time points (Figure 1D, bottom). To test if these changes are related, I plotted the average response rate at 30s versus the average response rate for the opposite, equidistant time point for the 100s omission trials, 70s, across training days. Correlation analysis revealed a strong relationship between the response rates at these times (Figure 2A: Pearson correlation coefficient, $R = -0.72$, $p = 0.0002$). In other words, increases in responding at 30s across training, appears to lead to lower response rates at 70s. Individual trial analysis based on raw press numbers confirmed this finding (Figure 2D, right: Pearson correlation coefficient, $R = -0.54$, $p = 0.0121$), thus excluding the possibility that the relationship was an artifact of the creation of the PETH. When I did this analysis for each second over the omission trial window, I was able to demonstrate that this relationship with the response rate at 30s persists from roughly 50-80s, further confirming the significance of the half peak fall time in the shaping of the peak (Figure 2B). Taken together, these results point to the possibility that response rates at one time point might have a bearing on dynamics that are not limited only to the time of responding.

Direct evidence for the relationship between response rate and 30s and fall time dynamics

also comes from training animals on SFI with no probe trials. When animals are trained on SFI with no probe trials and then switched to the regular 30% probe trial schedule on day 21, they show significantly lower response rates at 30s (Figure 2G, left: independent t-test, $p = 0.0241$) and delayed half peak fall times (Figure 2H: independent t-test, $p = 0.0002$) in probe trials compared to animals trained with 30% probe trials from day 1. It is important to note that both of these groups received exactly the same number of rewards at the same time each day with only the inclusion of probe trials during training differing. While it could be argued that these effects are the result of extinction from the introduction of reward omission trials on day 21, the response rates at 70s during omission trials on day 21 in the 100% rewarded training group are significantly higher (Figure 2G right: independent t-test, $p < 0.0001$) pointing to a lack of temporal control over action timing rather than simply a motivational effect.

Parts of chapter 2 are currently in preparation for submission for publication (Jonathan Cook, Bella Nguyen, Payaam Mahdavian, Megan Kirchgessner, Patrick Strassmann, Max Engelhardt, Edward M. Callaway, and Xin Jin). The dissertation author was the primary researcher and author of this material.

Figure 1. Self-paced fixed-interval timing behavior (A) The SFI schedule requires animals to both initiate and terminate the fixed-interval. For 70% of the trials, the first press 30s post-initiation yields a reward. Omission trials are randomly interleaved for the remaining 30% of the trials. (B) Operant chamber setup for SFI. (C) Response rasters of an exemplar for omission trials for day 1, 4, 7 and 21 under SFI training (top). PETHs can be calculated from the response rasters (middle) and divided by the maximum response rate for a given day to produce a percent maximum response rate PETH (bottom). SFI performance can be measured by the response rate at 30s (day 21 middle) and the half peak fall time (day 21 bottom) for omission trials. The peak time (day 21 bottom) is the amount of time post initiation to reach the maximum response rate in omission trials, which occurs around the time a reward would be delivered (30s). (D) Average PETHs (n = 10) for response rate (top) and percent maximum response rate (bottom). Values are mean ± SEM. (E-F) The presses per minute at 30s (E), half peak fall times and peak times (F), for days 1, 4, 7, 14 and 21 of SFI training (n = 10). Values are mean ± SEM. **** $p < 0.0001$; ** $p < 0.001$. n.s. denotes not significant; one-way ANOVA, Tukey's multiple comparisons.

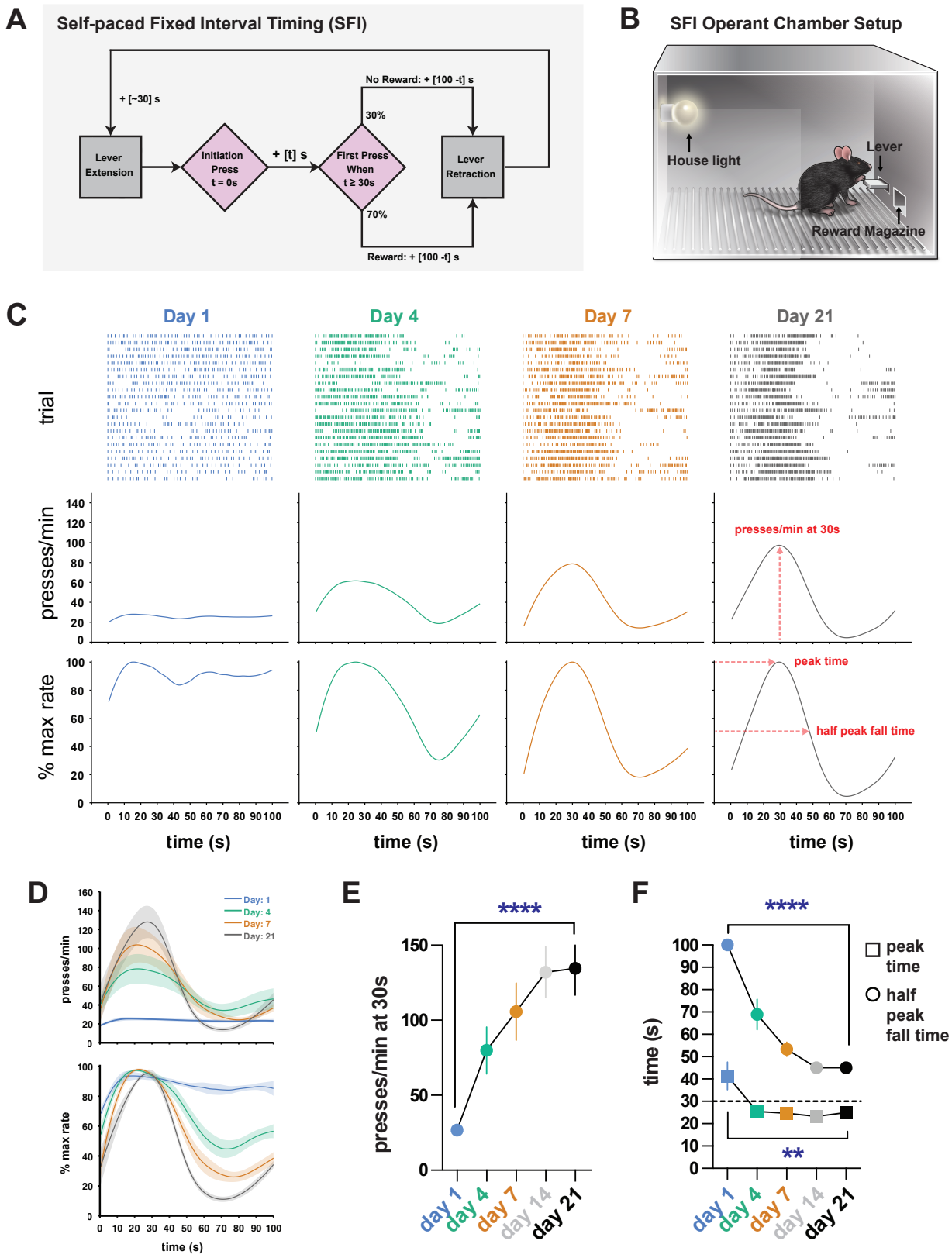
A
Self-paced Fixed Interval Timing (SFI)
+ [~30] s
Lever Extension
Initiation Press t = 0s
+ [t] s
First Press When t ≥ 30s
30%
No Reward: + [100 -t] s
70%
Reward: + [100 -t] s
Lever Retraction
B
SFI Operant Chamber Setup
House light
Lever
Reward Magazine
C
Day 1
Day 4
Day 7
Day 21
trial
presses/min
% max rate
presses/min at 30s
peak time
half peak fall time
time (s)
D
Day: 1
Day: 4
Day: 7
Day: 21
presses/min
% max rate
time (s)
E
****
presses/min at 30s
day 1
day 4
day 7
day 14
day 21
F
****
**
time (s)
peak time
half peak fall time
day 1
day 4
day 7
day 14
day 21

Figure 2. Response rates at 30s correlate to response rates at 70s across learning. (A) Correlation analysis of average response rate (n = 10) at 30s versus 70s based on PETH for omission trials. Grey, non-labeled points denote intermediate training days. Values are mean ± SEM. Grey shading, 95% confidence interval for regression. PCC denotes Pearson correlation coefficient. (B) The PCC can be calculated for the average response rate at each second over the omission trial window versus the average response rate at 30s across learning. The arrow denotes the correlation for 1A. (C-D) Trial-by-trial analysis for the number of presses from 20-30s and 60-70s confirms the relationship between responding at 30s and 70s from the response PETHs. (C) The response raster of an exemplar for the 5th trial of training days 1, 4, 7 and 21. (D) The number of responses over 20-30s for the same exemplar in 1C negatively correlates with the number of responses over 60-70s for the 5th trial (left). The average number of presses for all animals (n = 10) for the 5th trial over 20-30s negatively correlates with the average number of presses over 60-70s (right). Grey, non-labeled points denote intermediate training days. Values are mean ± SEM. Grey shading, 95% confidence interval for regression. PCC denotes Pearson correlation coefficient. (E-H) Comparison of day 21 SFI performance of animals with 70% rewarded trial training (n = 12) versus 100% rewarded trial training (n = 10). (E) Response rasters (top), response rate PETH (middle), and percent maximum response rate PETH (bottom) of exemplars for omission trials performing regular SFI (70% rewarded trials) on day 21 after being trained 20 days on either SFI with 70% (left) or 100% (right) rewarded trials. (F) Average PETHs for response rate (top) and percent maximum response rate (bottom) for day 21 of 70% rewarded and 100% rewarded training groups. (G) The response rate was lower at 30s (left) and higher at 70s (right) for the 100% rewarded training group relative to the 70% rewarded training group. (H) The half peak fall time was later in the 100% rewarded training group relative to the 70% rewarded training group, while there was no difference in the peak time. Values are mean ± SEM. * $p < 0.05$; *** $p < 0.01$; **** $p < 0.0001$. n.s. denotes non-significant; independent t-tests.

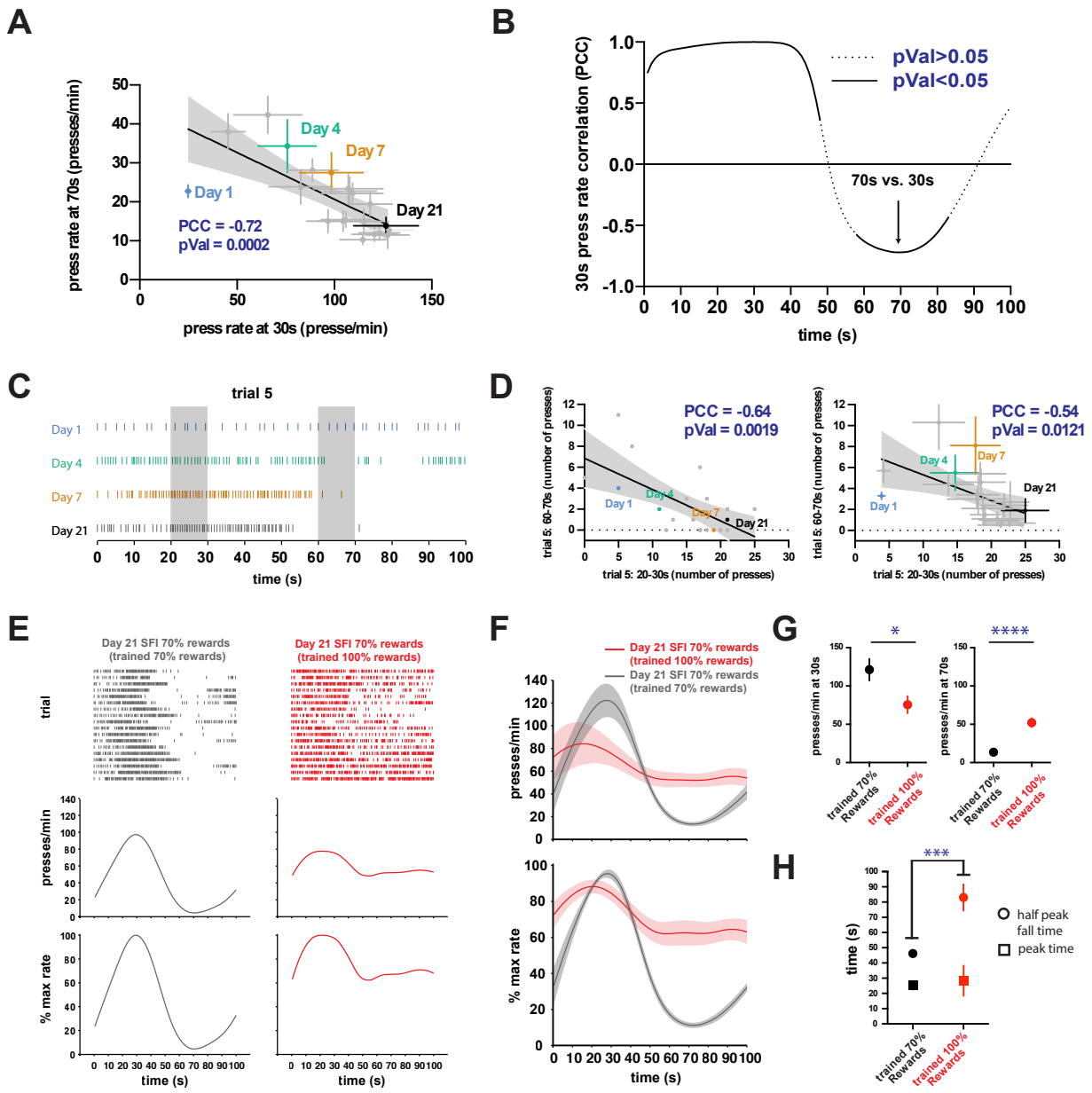
A
press rate at 70s (presses/min)
press rate at 30s (presse/min)
Day 1
Day 4
Day 7
Day 21
PCC = -0.72
pVal = 0.0002
B
30s press rate correlation (PCC)
time (s)
pVal>0.05
pVal<0.05
70s vs. 30s
C
trial 5
Day 1
Day 4
Day 7
Day 21
time (s)
D
trial 5: 60-70s (number of presses)
trial 5: 20-30s (number of presses)
PCC = -0.64
pVal = 0.0019
PCC = -0.54
pVal = 0.0121
E
Day 21 SFI 70% rewards
(trained 70% rewards)
Day 21 SFI 70% rewards
(trained 100% rewards)
trial
presses/min
% max rate
time (s)
F
Day 21 SFI 70% rewards
(trained 100% rewards)
Day 21 SFI 70% rewards
(trained 70% rewards)
presses/min
% max rate
time (s)
G
presses/min at 30s
presses/min at 70s
trained 70% Rewards
trained 100% Rewards
*
****
H
time (s)
half peak fall time
peak time
***

Chapter 3: A sensory role in self-paced fixed-interval timing performance

3.1 Acute sensory deprivation screen

Under SFI training, increases in responding at 30s and overall timing dynamics seem to be acquired in tandem across learning, implying that responding itself might play an implicit role in how animals produce dynamic press distributions, consistent with BET (Killeen and Fetterman, 1988; Machado, 1997). If animals were indeed relying on the action state at one time point to inform future action, one possibility is that a sensorimotor mechanism is being employed to shape timing dynamics. To test this idea, I performed three-day, acute sensory deprivation experiments testing three modalities that could potentially inform animals of ongoing action: vision, audition and proprioception/somatosensation. If a sensory feedback mechanism was being employed, it would be expected that decoupling the modality tuned to action should disrupt SFI performance.

Following 21 days of training on SFI, sensory deprivation manipulation experiments were performed over an entire session between 2 flanking control sessions (pre-control and post-control). In the first experiment, I tested somatosensation/proprioception, by injecting a lidocaine/CNQX cocktail into the brachial plexus behind the left and right scapula (Figure 2A). This nerve block has the effect of stopping neurotransmission of both afferent and efferent nerve fibers to the forearm, meaning that motor control and all forms of somatosensation and proprioception are attenuated (Koch et al., 2017). This manipulation showed a modest, almost significant, decrease in response rate at 30s (Figure 2A left: one-way ANOVA, $F_{(2,18)} = 3.99$, $p = 0.0368$, Tukey's multiple comparison test, pre-control vs. manipulation, $p = 0.0501$) but no disruption in half peak fall time or peak time (Figure 2A, right). The role of the visual system in SFI performance was tested by simply turning off the operant chamber house light (Figure 2B).

As with the proprioception/somatosensation manipulation, no effect on SFI performance in terms of response rate eat 30s (Figure 2B, left) nor half peak fall time or peak time was observed (Figure 2B, right).

Next, I tested the role of audition in SFI (Figure 2C). Bilateral ear sealing profoundly disrupted SFI performance. Auditory deprivation resulted in a large decrease in responding at 30s compared to day -1 levels (Figure 2C, left: one-way ANOVA, $F_{(2,18)} = 10.88$, $p = 0.0008$, Tukey's multiple comparison test, pre-control vs. manipulation, $p = 0.0008$). Peak dynamics were also disrupted with a delay in the half peak fall time (Figure 2C, right: one-way ANOVA, $F_{(2,18)} = 35.78$, $p < 0.0001$, Tukey's multiple comparison test, pre-control vs. manipulation, $p < 0.0001$). No effect on the peak time was observed. The sensory deprivation effect was mostly specific to the day of manipulation with average 30s response rates and half peak fall times in the following control day returning to pre-control levels. The effects of the ear sealing on hearing were assayed via measuring the acoustic startle reflex to a 40ms, 120 dB auditory stimulus (Crawley et al., 1997). With ear sealing animals showed ~75% attenuated startle amplitude (Figure 2D; one-way ANOVA, $F_{(2,10)} = 8.66$, $p = 0.0066$, Tukey's multiple comparison test, pre-control vs. manipulation, $p = 0.0060$).

3.2 What are the mice listening to?

It is difficult to say precisely what auditory stimulus is being utilized in the performance of SFI. One possibility is that auditory deprivation is disrupting a conditioned auditory cue related to reward delivery, such as the sound of the pellet dropping into the reward magazine. If animals had indeed learned to utilize an auditory cue signaling reward delivery, it is possible that disrupting hearing could exert effects on SFI performance via an altered motivational or attentional state associated with hearing, or expecting to hear this cue. To exclude this

possibility two separate groups of animals underwent extinction in which they were exposed to continuous probe trials. Peak performance was largely intact under extinction with ears open and comparison to the separate ear sealed extinction group still revealed significant effects on response rate at 30s (Figure 4A, left: independent t-test, $p = 0.0001$) and half peak fall time (Figure 4A, right: independent t-test, $p = 0.0041$), but no changes in peak time.

In probe trials, the only sound present comes from the animal physically interacting with the lever. Pressing the lever results in a very salient clicking sound (Figure 4D) that generates a ~50 ms auditory stimulus (Figure 4E, right) with 5000 Hz and 10000 Hz peak amplitude components (Figure 4E-F), resulting from the internal mechanism of the lever making contact with its housing. I suspected that this sound was the most likely candidate to explain the auditory-dependent behavioral effects I observed that could be explained within the context of the extinction results, where no other auditory cues are available for the animal to use. I next asked how the auditory system itself responds when animals are performing SFI. If animals were indeed learning to listen to their own self-generated sound to inform motor timing, it would be expected that neural responses in auditory brain structures would reflect this sensorimotor relationship.

Parts of chapter 3 are currently in preparation for submission for publication (Jonathan Cook, Bella Nguyen, Payaam Mahdavian, Megan Kirchgessner, Patrick Strassmann, Max Engelhardt, Edward M. Callaway, and Xin Jin). The dissertation author was the primary researcher and author of this material.

Figure 3. Auditory deprivation acutely disrupts SFI performance (A-C) Response rates at 30s (left) and half peak fall and peak times (right) for omission trials of thee-day sensory manipulation experiments testing somatosensation/ proprioception (n = 10) (A), vision (n = 10) (B), and audition (n = 10)(C). Deprivation sessions (manipulation) were performed between flanking control sessions (pre-control and post-control). Values are mean ± SEM; ** $p < 0.01$; *** $p < 0.001$; ****$p < 0.0001$. n.s. denotes not significant; one-way ANOVA, Tukey's multiple comparisons. (D) Startle amplitude in response to a 40 ms, 120 dB auditory stimulus (n = 7) during ear sealing and flanking control sessions (pre-control and post-control). Values are mean ± SEM. * $p < 0.05$; ** $p < 0.01$. n.s. denotes not significant; one-way ANOVA, Tukey's multiple comparisons (E) Response rasters (top), response rate PETH (middle) and percent maximum response rate PETH (bottom) of an exemplar for omission trials performing SFI under auditory deprivation (ear seal) between flanking control sessions (pre-control and post-control). (F) Average PETHs for response rate (top) and percent maximum response rate (bottom) for pre-control session and ear seal (n = 10). Values are mean ± SEM.

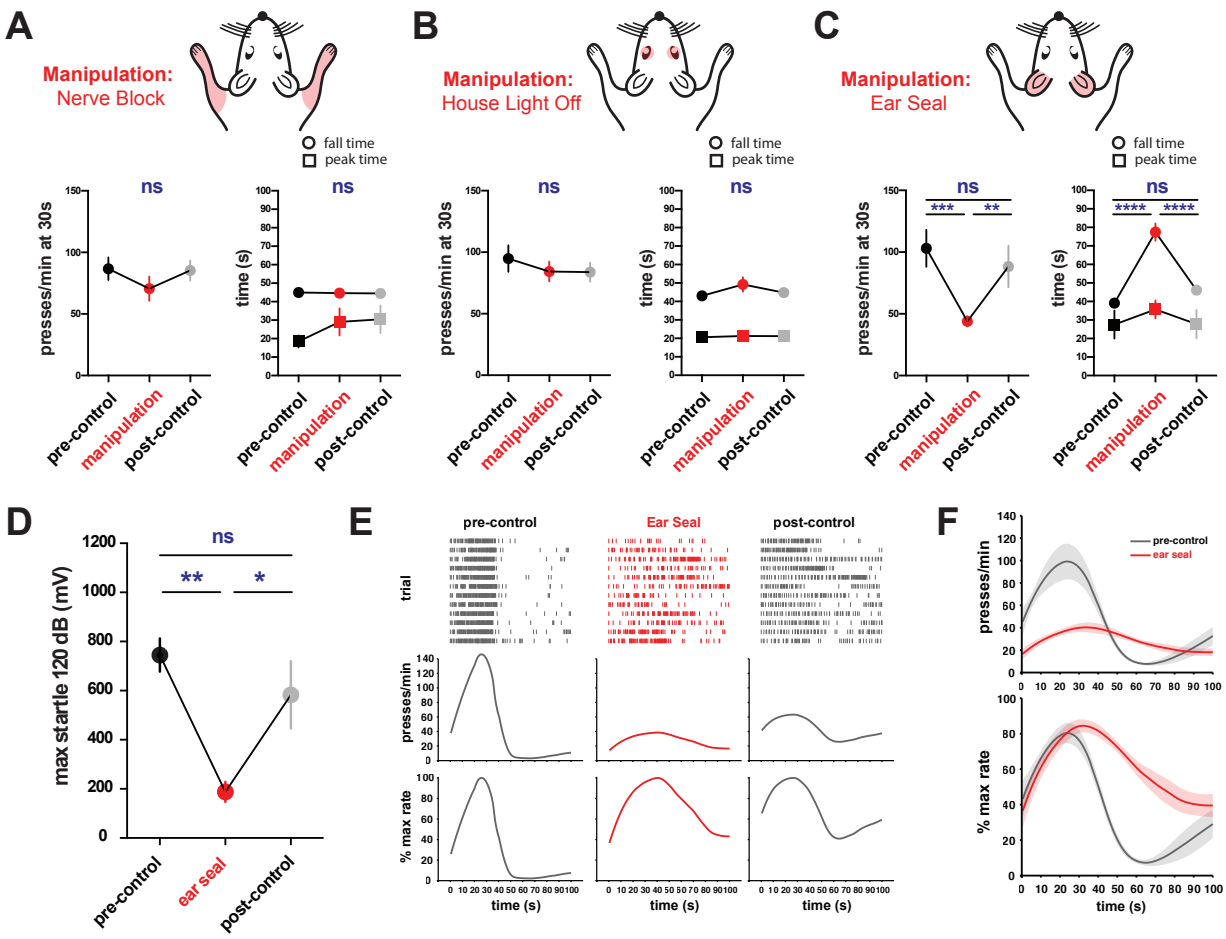
A
Manipulation:
Nerve Block
fall time
peak time
presses/min at 30s
time (s)
ns
pre-control
manipulation
post-control
B
Manipulation:
House Light Off
C
Manipulation:
Ear Seal
***
**
****
D
max startle 120 dB (mV)
**
*
ear seal
E
pre-control
Ear Seal
post-control
trial
presses/min
% max rate
time (s)
F
pre-control
ear seal
presses/min
% max rate
time (s)

Figure 4. SFI extinction and lever pressing auditory stimulus. (A-C) Separate groups of animals underwent extinction through exposure to continuous omission trials with ears open (n = 8) or sealed (n = 10). (A) Response rate at 30s (left), half peak fall time and peak time (right) for extinction trials. Values are mean ± SEM. **p < 0.005; ****p < 0.0001; independent t-tests. (B) Response rasters (top), response rate PETH (middle) and percent maximum response rate PETH (bottom) of exemplars for omission trials performing extinction post-21 days of training on SFI with ears open (left) and sealed (right). (C) Average PETHs for response rate (top) and percent maximum response rate (bottom) for ears sealed and open groups. Values are mean ± SEM. (D) Response raster from a single probe trial (top) and audio recording signal (bottom) showing responding elicits an auditory stimulus. (E) Audio spectrogram for 0.2s bin containing a press (left) and no press (right) from probe trial recording in (D). (F) Power spectral density periodogram for the 0.2s bins containing the press and no press in (E) shown zoomed in inset.

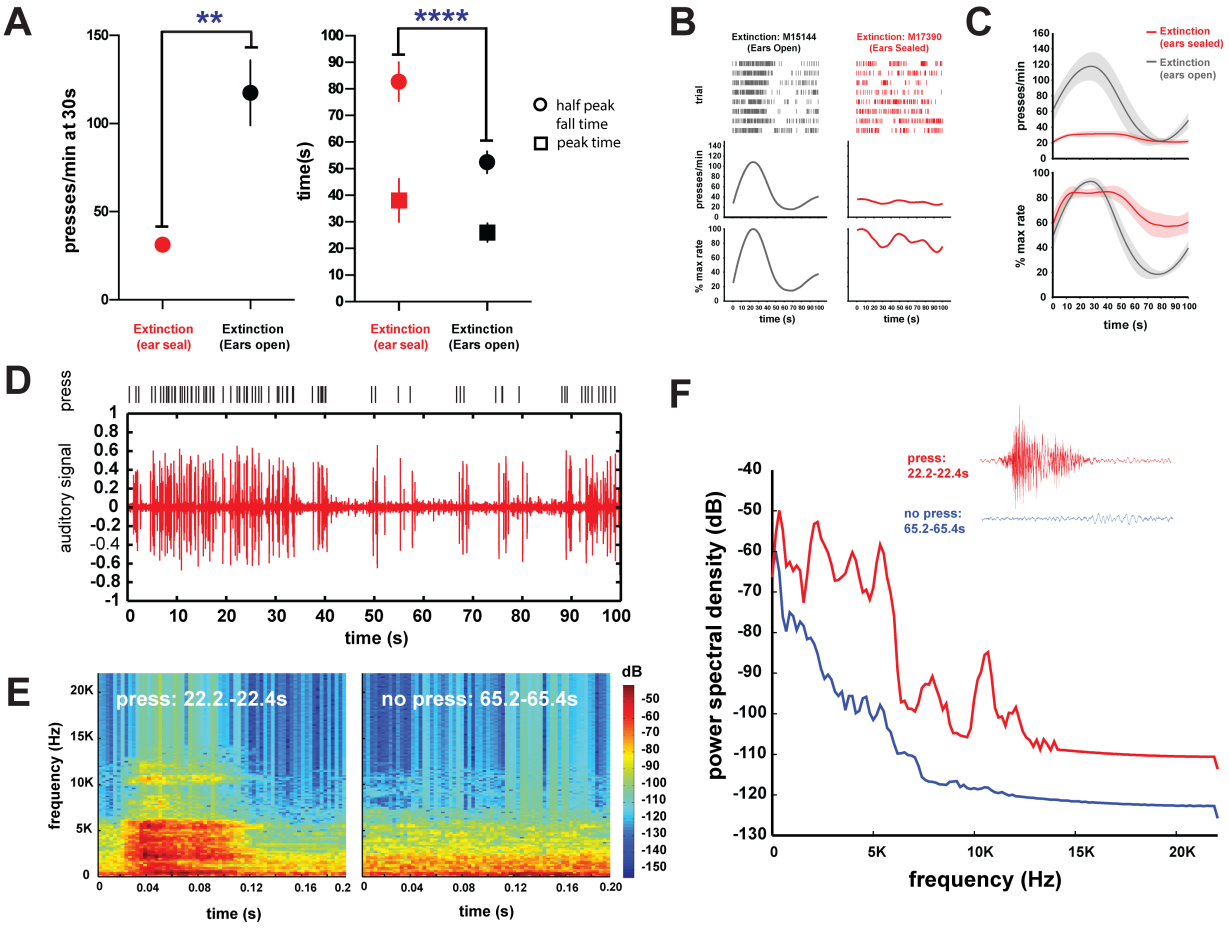
A
**
****
presses/min at 30s
time(s)
half peak
fall time
peak time
Extinction (ear seal)
Extinction (Ears open)
Extinction (ear seal)
Extinction (Ears open)
B
Extinction: M15144 (Ears Open)
Extinction: M17390 (Ears Sealed)
trial
presses/min
% max rate
time (s)
C
Extinction (ears sealed)
Extinction (ears open)
presses/min
% max rate
time (s)
D
press
auditory signal
time (s)
E
press: 22.2.-22.4s
no press: 65.2-65.4s
frequency (Hz)
time (s)
dB
F
press: 22.2-22.4s
no press: 65.2-65.4s
power spectral density (dB)
frequency (Hz)

Chapter 4: A neural substrate for sensing action in task performance

4.1 The dorsal auditory cortex and performance

To test the idea that the auditory system shows response properties related to pressing, I performed an immunohistochemistry screen with the immediate early protein, cFos, on animals that performed SFI. Comparing the cFos expression pattern of bilaterally sealed animals versus animals with their ears open is problematic. Bilaterally sealing substantially disrupts SFI peak performance and almost all auditory sensory input is essentially blocked. Random, unilateral sealing (Figure 5A) results in moderate effects on the press rate at 30s (Figure 5B, left: one-way ANOVA, $F_{(2,25)} = 17.80$, $p < 0.0001$, Tukey's multiple comparison test, open vs. unilateral, mean difference = 57.90 presses/min, $p < 0.0030$; open vs. bilateral, mean difference = 86.80 presses/min, $p < 0.0001$) and half peak fall times (Figure 3B, right: one-way ANOVA, $F_{(2,25)} = 27.01$, $p < 0.0001$, Tukey's multiple comparison test, open vs. unilateral, mean difference = 13.38 s, $p = 0.0369$; open vs. bilateral, mean difference = 34.95 s, $p < 0.0001$) compared to animals with their ears open. I hypothesized that a neural locus receiving unilateral auditory input might differentially express cFos across the two hemispheres and allow for the determination of an area related to the observed auditory-dependent behavioral effects. Following 21 days of training on SFI, animals had a single ear randomly sealed , and were then allowed to perform SFI. Upon completion of the session under unilateral auditory deprivation, animals were immediately sacrificed for cFos immunohistochemical analysis (Figure 3C).

I examined cFos expression in the three major auditory regions of the cortex: AuDd (Figure 5C, left), primary auditory cortex (AuDp, Figure 5C, middle) and the ventral auditory cortex (AuDv, Figure 5C, right). Calculating the percentage of cells across the two hemispheres (open and sealed) for a particular region, revealed a higher activation in AuDd for the hemisphere ipsilateral to the open ear (Figure 5D: two-way ANOVA, $F_{(2,24)} = 3.69$, $p = 0.0402$,

Sidak's multiple comparison test, AuDd open vs. sealed, p = 0.0003). AuDp and AuDv showed no percent difference in cFos expression across the two hemispheres with regard to sealing. Breaking down AuDd into layers, I determined that layer V of AuDd was primarily responsible for this hemispheric imbalance in activation (Figure 5E: two-way AVOVA, $F_{(4,40)} = 2.96$, p = 0.0313, Sidak's multiple comparison test, AuDd layer V: open vs. sealed, p = 0.0005). Since the sealed ear was randomly selected and higher activation was always observed in the hemisphere ipsilateral to the open ear, the observed hemispheric imbalance could not be explained by motor cortex corollary discharge, but rather sensory input (Schneider et al., 2014).

4.2 The dorsal auditory cortex shows press-dependent activation

The behavioral extinction experiments strongly pointed toward the sound generated from lever pressing as the most likely stimulus to explain the auditory deprivation effects on SFI performance. Thus, I decided to test the role of lever pressing on the observed hemispheric activation imbalance in AuDd resulting from unilateral sealing. I redid the unilateral ear sealing experiment on day 1 of SFI training, when lever press rates at 30s are much lower than day 21 (Figure 1E), and found that activation across the two hemispheres according to cFos expression (Figure 5F, top) was not significantly different (Figure 5G). Furthermore, I trained animals to day 20 on SFI and removed the lever on day 21, keeping all other aspects of the task in tact. Under this lever omitted version animals still received rewards and had interleaved probe trials, but with task progression and pellet delivery occurring in a manner as if the animal were continually pressing the lever had it been present. Again, unilateral ear sealing under this lever-omitted version did not result in differences in cFos activation (Figure 5F, bottom) across the two hemispheres (Figure 5G). I calculated a cFos activation ratio as the dividend of the total cells in the hemisphere ipsilateral to the open ear divided by the total cells in the hemisphere ipsilateral

to the sealed ear for AuDd for the three lever testing conditions: SFI day 1 (lever present), day 21 (lever present) and day 21 (lever absent). Plotting these values against the corresponding press rates at 30s for each animal on the day they were sacrificed revealed a significant linear relationship, in which higher activation ratios were associated with higher press rates (Figure 5H: Pearson correlation coefficient = 0.65, $p = 0.0084$).

Parts of chapter 4 are currently in preparation for submission for publication (Jonathan Cook, Bella Nguyen, Payaam Mahdavian, Megan Kirchgessner, Patrick Strassmann, Max Engelhardt, Edward M. Callaway, and Xin Jin). The dissertation author was the primary researcher and author of this material.

Figure 5. AuDd shows press-dependent cFos expression during SFI performance. (A) Schedule for cFos screening experiments for animals with a unilateral ear seal during SFI performance. (B) Comparison of press rate at 30s (left) and half peak fall times and peak times (right) for animals trained on SFI with unilateral ear seal (n = 8), bilateral ear seal (n = 10) versus no ear seal (n = 10). Values are mean ± SEM. * $p < 0.05$; ** $p < 0.005$; **** $p < 0.0001$. n.s. denotes not significant; one-way ANOVA, Tukey's multiple comparisons. (C) cFos immunohistochemistry for exemplars showing AuDd (left), AuDp (middle) and AuDv (right) cortical regions for animals sacrificed on day 21 of SFI training with one ear randomly sealed (left) and one ear open (right). Scale bar denotes 50 μm. "D" denotes dorsal and "L" denotes lateral. (D) Comparison of percent activation according to cFos counts across hemispheres for each AuD cortical region ipsilateral versus contralateral to the sealed ear of animals sacrificed upon completion of SFI at day 21 (n = 5) of training. Bars are mean. *** $p < 0.0005$. n.s. denotes not significant; two-way ANOVA, Sidak's multiple comparisons. (E) Comparison of percent activation according to cFos counts across hemispheres for cortical layers in AuDd ipsilateral versus contralateral to the sealed ear of animals sacrificed upon completion of SFI at day 21 (n = 5) of training. Bars are mean. *** $p < 0.001$. n.s. denotes not significant; two-way ANOVA, Sidak's multiple comparisons. (F) cFos immunohistochemistry for exemplars showing AuDd for an animal with one ear randomly sealed (left) and one ear open (right) on day 1 of SFI training (top) and another animal that performed the lever omitted version of the task on day 21 after being trained 20 days of regular SFI (bottom). Scale bar denotes 50 μm. "D" denotes dorsal and "L" denotes lateral. (G) Comparison of percent activation across hemispheres for AuDd ipsilateral versus contralateral to the sealed ear according to cFos counts for animals sacrificed on SFI training day 1 (n = 5) and day 21 of the lever omitted version after 20 days on regular SFI (n = 5). Bars are mean. n.s. denotes not significant; two-way ANOVA, Sidak's multiple comparisons. (H) Activation ratios (number of cells in hemisphere ipsilateral to the open ear ÷ number of cells in hemisphere ipsilateral to the sealed ear) plotted against the press rate at 30s of each individual animal on the day of sacrifice for day 21 of the lever omitted version after 20 days on regular SFI and days 1 and 21 of regular SFI. Grey shading, 95% confidence interval for regression. PCC denotes Pearson correlation coefficient.

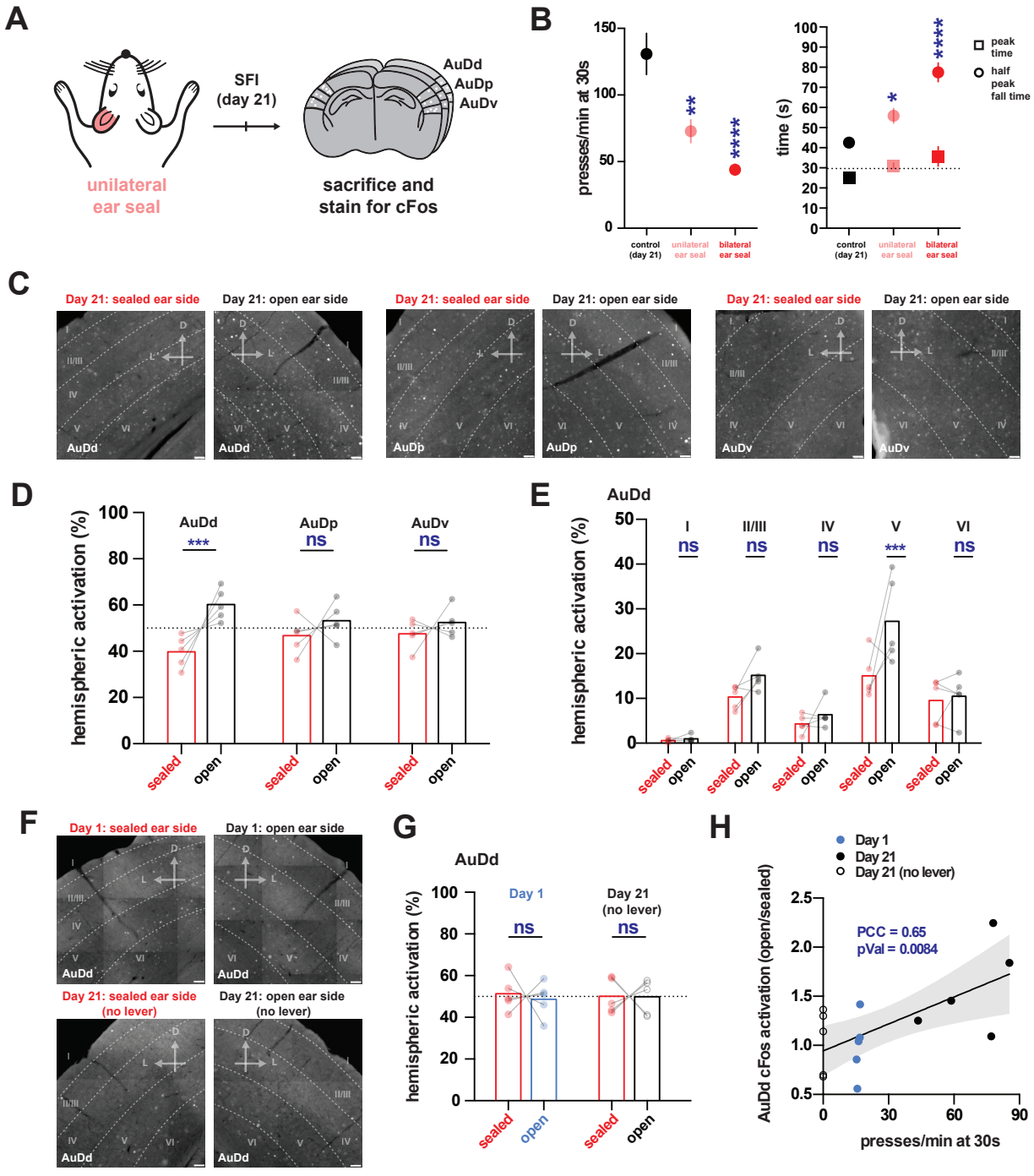
A
unilateral
ear seal
SFI
(day 21)
AuDd
AuDp
AuDv
sacrifice and
stain for cFos
B
presses/min at 30s
time (s)
peak
time
half
peak
fall time
control
(day 21)
unilateral
ear seal
bilateral
ear seal
C
Day 21: sealed ear side
Day 21: open ear side
AuDd
AuDp
AuDv
D
hemispheric activation (%)
AuDd
AuDp
AuDv
ns
sealed
open
E
AuDd
I
II/III
IV
V
VI
F
Day 1: sealed ear side
Day 1: open ear side
Day 21: sealed ear side
(no lever)
Day 21: open ear side
(no lever)
G
Day 1
Day 21
(no lever)
H
Day 1
Day 21
Day 21 (no lever)
PCC = 0.65
pVal = 0.0084
AuDd cFos activation (open/sealed)
presses/min at 30s

Chapter 5: Sensorimotor feedback control in task performance

5.1 Muscimol inactivation of the auditory cortex

The cFos screen and the relationship discovered between lever pressing and activation of AuDd led us to ask if this cortical region was necessary for SFI task performance. Inactivation of the auditory cortex (including AuDd) via infusion of the selective agonist for $GABA_A$, muscimol (Figure 6C, top left), resulted in a decrease in the response rate at 30s (Figure 6C, top middle: paired t-test, saline vs. muscimol, $p = 0.0203$) and increase in the half peak fall time (Figure 6C, top right: paired t-test, saline vs. muscimol, $p = 0.0272$), strongly resembling the effects observed with acute auditory deprivation. As a point, of comparison to the auditory cortex inactivation, I also performed muscimol infusions in the visual cortex (Figure 6C, bottom left). Consistent, with the sensory deprivation screen, there was no significant effect on response rate at 30s (Figure 6C, bottom middle) or half peak fall time (Figure 6C, bottom right).

5.2 Activity-dependent labeling in the dorsal auditory cortex

In order to more directly address a causal relationship between auditory cortex activation, lever responding and auditory-dependent SFI performance, I utilized a genetic, activity-dependent labeling method, TRAP, or targeted recombination of active populations (Guenthner et al., 2013), in conjunction with a closed-loop optical stimulation feedback system. The FosTRAP animal exploits the promoter of cFos, to drive the expression of tamoxifen sensitive Cre-recombinase in an activity-dependent manner. Following 21 days of SFI training, FosTRAP animals were allowed to perform SFI either with their ears open or sealed and received an intraperitoneal injection of 4-hydroxytamoxifen (4-OHT) midsession. 4-OHT was used in place of tamoxifen, as it is more metabolized and allows for a narrower time window for activity-dependent labeling. Prior to 4-OHT induction with ears open or sealed, animals were injected with an AAV in AuDd expressing channelrhodopsin (ChR2) in either a Cre-on or Cre-off-

dependent manner (Figure 6D).

5.3 Press-triggered optical stimulation under auditory deprivation

I asked if press-dependent optical activation of the labeled active population in the auditory cortex under auditory deprivation could rescue some of the SFI response dynamics lost with ear sealing. Induced FosTRAP animals, injected with ChR2 and implanted with optical fibers in AuDd, performed an optical-intracranial self-stimulation (opto-ICSS) version of SFI under auditory deprivation. Opto-ICSS SFI (Figure 6E) was identical to regular SFI, except that lever pressing resulted in 100 ms of constant (Figure 6F), 5 mW blue light delivery to AuDd in 50% of probe and rewarded trials. Importantly, for stimulated probe and rewarded trials, optical feedback occurred for any press when the lever was available for responding and was not limited to any particular time window, thus preventing stimulation itself from serving as a temporally discriminative cue.

I tested three conditions with FosTRAP using opto-ICSS SFI under auditory deprivation: (1) 4-OHT induction performed with ears open and Cre-on-dependent ChR2 expression in AuDd (4-OHT/open/on, Figure 6G, top), (2) 4-OHT induction with ears sealed and Cre-on-dependent Chr2 in AuDd (4-OHT/sealed/on, Figure 6G, middle) and (3) 4-OHT induction with ears open and Cre-off-dependent ChR2 in AuDd (4-OHT/open/off, Figure 6G, bottom). The first and the second experimental conditions tested the active population's sensory feedback role in SFI performance and its induction-dependency on auditory input, with the assumption that a rescue effect would be observed only under the condition that the ears were open during 4-OHT induction. The third experimental condition tested the specificity of the active population in its ability to influence SFI performance. If the population's role in SFI performance was genetically specific, then rescue effects should not be observed in animals labeling the inverse of the active

population.

Optical stimulation trials had significantly higher press rate at 30s (Figure 6H, left: two-way ANOVA, $F_{(2,37)} = 8.23$, $p = 0.0011$, Sidak's multiple comparison test, ear sealed no stimulation vs. ear sealed stimulation, $p = 0.0009$) and decreases in half peak fall times (Figure 6H, middle: two-way ANOVA, $F_{(2,37)} = 4.13$, $p = 0.0241$, Sidak's multiple comparison test, ear sealed no stimulation vs. ear sealed stimulation, $p = 0.0194$) compared to the trials with no optical feedback for 4-OHT/open/on animals performing opto-ICSS SFI under ear sealing. These optogenetic effects appeared to behaviorally specific, with other task performance features, such as head entry rate at 30s (Figure 6M) and rewarded head entry time (Figure 6L), not showing any difference between stimulated and non-stimulated trials. In contrast to the 4-OHT/open/on animals, optical stimulation resulted in no change in response rates at 30s (Figure 6H, left) and half peak fall times (Figure 6H, middle) compared to non-stimulation trials for 4-OHT/sealed/on and 4-OHT/open/off animals performing opto-ICSS SFI under auditory deprivation. No significant interaction was observed in regards to the effect of optical stimulation on peak time for the three conditions tested (Figure 6H, right).

For 4-OHT/open/on animals, the improvement effects on press rate and fall dynamics varied, with some animals experiencing larger optogenetic rescues than others. One possibility is that these effects are mutually dependent, as demonstrated in SFI learning, meaning large increases in presses rates are associated with earlier fall times. However, it is also possible that these effects are mutually exclusive, meaning that optically induced press rate increases do not necessarily relate to better fall time dynamics, or in other words, the rescue effects on press rate are not specific to a particular time window over probe trials. If optical stimulation was simply providing a generalized motor effect, lever pressing would be expected to increase broadly

across the entire probe trials. On the other hand, if the self-stimulation was influencing the timing of responses, then increases in pressing would be expected to be temporally specific and thus correlate with earlier half peak fall times. I asked how the changes in press rates at 30s related to changes in the observed decreases in fall times and found a significant negative correlation for the 4-OHT/open/on condition (Figure 6I, left: Pearson correlation coefficient = -0.72, $p < 0.0048$), such that animals that experienced the largest changes in press rates at 30s also experienced the largest changes in half peak fall times. For the other two conditions, 4-OHT/sealed/on (Figure 6I, middle) and 4-OHT/open/off (Figure 6I, right), this constructive effect between changes in press rate and fall time dynamics was not observed.

To validate the ability of the FosTRAP animal to faithfully express Cre in a manner consistent with endogenous cFos protein expression, I looked at the distribution of cFosCre positive cells across the cortical layers of AuDd compared to the distribution of the cFos protein itself (Figure 7). FosTRAP animals were injected with an AAV into AuDd expressing GFP in a Cre-dependent manner and induced with their ears open while performing SFI following 21 days of training. 10 days later, the same animals performed SFI again with their ears open and were immediately sacrificed upon session completion (Figure 7A, top). The AuDd expression distributions across cortical layers for GFP and cFos protein in this double labeling experiment were compared to the distribution of cFos protein from a separate group of FosTRAP animals trained on SFI that completed the no lever version of the task with their ears open and immediately sacrificed upon session completion (Figure 7A, bottom). The cFos protein and cFosCre expression patterns (Figure 7C and 7E) showed no difference in their percent distributions across the cortical layers for the double labeling experiment (Figure 7B). In contrast, the no lever group (Figure 7D) had a cFos protein expression pattern that was

significantly blunted in layer V (Figure 7B: two-way ANOVA, $F_{(8,45)} = 2.335$, $p = 0.0343$, Tukey's multiple comparison test, Layer V: cFosCre SFI vs. cFos no lever, $p = 0.0172$; cFos SFI vs. cFos no lever, $p = 0.0496$). This result demonstrates a unique cFos protein cortical activation profile in AuDd that is specific to SFI task performance and can be recapitulated using the FosTRAP animal. This result is also consistent with the unilateral ear sealing experiments, which demonstrate an acute affect on layer V activation (Figure 5E).

5.4 Physiological effects of stimulating labeled populations

To determine the physiological effects of AuDd optical stimulation that underlie the observed behavioral effects, single-units in AuDd were recorded extracellularly from a separate group of 4-OHT/open/on and 4-OHT/open/off FosTRAP animals (Figure 8). Units with significant short latency (<10ms, SALT $p<.01$; (Kvitsiani et al., 2013) responses to 100ms light pulses were recorded in 4-OHT/open/on (Figure S3A) and 4-OHT/open/off animals (Figure S3D), but with much higher prevalence in the 4-OHT/open/off animals (Figure 8C and 8F: 17% Cre-on vs. 79% Cre-off), which is qualitatively consistent with the levels of ChR2 expression observed in the two groups and their expected combined proportions (i.e. ~100%). Optical stimulation resulted in increased activity during the full 100ms of optical stimulation in most putatively photo-tagged units in both groups (Figure 8B and 8E), but the distribution of these units differed; most photo-tagged units in the 4-OHT/open/on animals were recorded at depths corresponding to the infragranular layers (Figure 8C), but in the 4-OHT/open/off group they were more evenly distributed across cortical depth (Figure 8F). While this demonstrates that selective ChR2-expressing populations were effectively manipulated by the optical stimulation protocol, the population-level effects of selective Cre-on vs. Cre-off optical stimulation differed substantially. Cre-off stimulation dramatically increased spiking activity across cortical depths

(Figure 8F), whereas the effect of Cre-on stimulation was largely suppressive (Figure 8C). Thus, while optical stimulation of non-Cre-expressing populations results in non-specific facilitation of activity in AuDd, stimulation of Cre-expressing populations facilitates the activity of those populations specifically, but suppresses the rest of the network. If one considers the Cre-expressing populations as representing components of an auditory "signal" that are important for the animals' performance of the task, while the activity of non-Cre-expressing populations are irrelevant to the task, or "noise", the selective facilitation with widespread suppression observed in the Cre-on animals can be likened to an improvement in AuDd signal-to-noise. This is reminiscent of what has been observed in mice engaged in an auditory task (Otazu et al., 2009) and in non-human primates during self-initiated vocalizations (Eliades and Wang, 2008).

5.5 Contribution of layer V

The unilateral auditory deprivation experiments and cFos staining results demonstrated an acute affect on layer V AuDd activation (Figure 5E and 7B). Projections from layer V of the auditory cortex to the striatum have been found to mediate auditory-based action selection (Znamenskiy and Zador, 2013). Furthermore, striatal populations have been shown to control response dynamics in fixed-interval timing tasks (Drew et al., 2007; Ward et al., 2009). Consequently, I wanted to address the contribution of the active populations in Layer V of AuDd in SFI performance. To do this I used a viral-based activity-dependent labeling system using ESARE, or enhanced synaptic activity-responsive element. ESARE is a synthetic activity-responsive element that uses the promoter of the immediate early gene Arc. I packaged ESARE-ERCreER-PEST as the retrograde AAV serotype, rAAV2, and injected the virus into the dorsal medial striatum (DMS) of C57BL6 animals with a Cre-dependent AAV in AuDd expressing ChR2 (Figure 9A). Following surgery and training animals were induced using 4-OHT while

performing SFI with their ears open. Using this strategy, I was able to isolate active populations in layer V of AuDd (Figure 9B) projecting to the striatum (Figure 9C). As with the FosTRAP experiments in AuDd, I performed opto-ICSS SFI in these ESARE injected animals under auditory deprivation. Stimulating these layer V populations in AuDd was sufficient to increase the response rate at 30s (Figure 9D, left: paired t-test, $p = 0.0438$) and also caused a concurrent decrease in the half peak fall time (Figure 9D, middle: paired t-test, $p = 0.0277$), with no changes in the peak time.

Parts of chapter 5 are currently in preparation for submission for publication (Jonathan Cook, Bella Nguyen, Payaam Mahdavian, Megan Kirchgessner, Patrick Strassmann, Max Engelhardt, Edward M. Callaway, and Xin Jin). The dissertation author was the primary researcher and author of this material.

Figure 6. Feedback control of SFI response dynamics via AuDd active population (A) Response rasters (top), response rate PETH (middle) and percent maximum response rate PETH (bottom) of an exemplar for omission trials performing SFI with saline infusion (pre-control) and muscimol infusion. (B) Average PETHs for response rate (top) and percent maximum response rate (bottom) for pre-control session (saline) and muscimol infusion in the auditory cortex (n = 5). Values are mean ± SEM. (C) Inactivation of the auditory cortex via muscimol infusion (top left) results in a decrease in responding at 30s (top middle), an increase in half peak fall time and no change in peak time (top right) (n = 5). Inactivation of the visual cortex via muscimol infusion (bottom left) results in no change in press rate at 30s, (bottom middle) half peak fall time or peak time (bottom right) (n = 6). Values are mean ± SEM. * $p < 0.05$; n.s. denotes not significant; paired t-tests. (D-K) Press-dependent optical activation of labeled active populations in AuDd can partially rescue sensorimotor features of SFI response dynamics lost under auditory deprivation. (D) Trained FosTRAP animals were induced via intraperitoneal injection of 4-OHT with either their ears sealed or open while performing SFI after being injected with a Cre-on/off-dependent AAV expressing ChR2 and implanted with optical fibers. (E) Opto-ICSS SFI was identical to regular SFI, except 50% of probe and rewarded trials resulted in 100ms of constant blue light being delivered intracranially with each lever press. (F) Operant chamber setup for opto-ICSS SFI. (G) Exemplar expression patterns in AuDd of ChR2 in the three experimental conditions tested with FosTRAP: 4-OHT/open/on (top), 4-OHT/sealed/on (middle) and 4-OHT/open/off (bottom). (H) Opto-ICSS SFI response rates at 30s (left), half peak fall times (middle) and peak time for optical stimulation and no stimulation omission trials in the three experimental conditions tested with FosTRAP: 4-OHT/open/on (n = 14), 4-OHT/sealed/on (n = 13) and 4-OHT/open/off (n = 13). Bars are mean. * $p < 0.05$; *** $p < 0.001$. n.s. denotes not significant; two-way ANOVA, Sidak's multiple comparisons. (I) Correlational analysis of change in the press rate at 30s and change in half peak fall time between stimulation and no stimulation trials (Δ = stimulation − no stimulation) for the three experimental conditions tested with FosTRAP: 4-OHT/open/on (left), 4-OHT/sealed/on (middle) and 4-OHT/open/off (right). Grey shading, 95% confidence interval for regression. n.s. denotes not significant. PCC denotes Pearson correlation coefficient. (J) Response rasters for stimulation and no stimulation trials (top), response rate PETHs (middle) and percent maximum response rate PETHs (bottom) of a 4-OHT/open/on exemplar for omission trials performing opto-ICSS SFI. (K) Stimulation and no stimulation average PETHs for response rate (top) and percent maximum response rate (bottom) for opto-ICSS SFI omission trials for the 4-OHT/open/on condition (n = 14). Values are mean ± SEM. Rewarded head entry time (L) and head entry rate at 30s (M) for stimulation and no stimulation omission trials for the 4-OHT/open/on condition (n = 14). n.s. denotes not significant; paired t-tests.

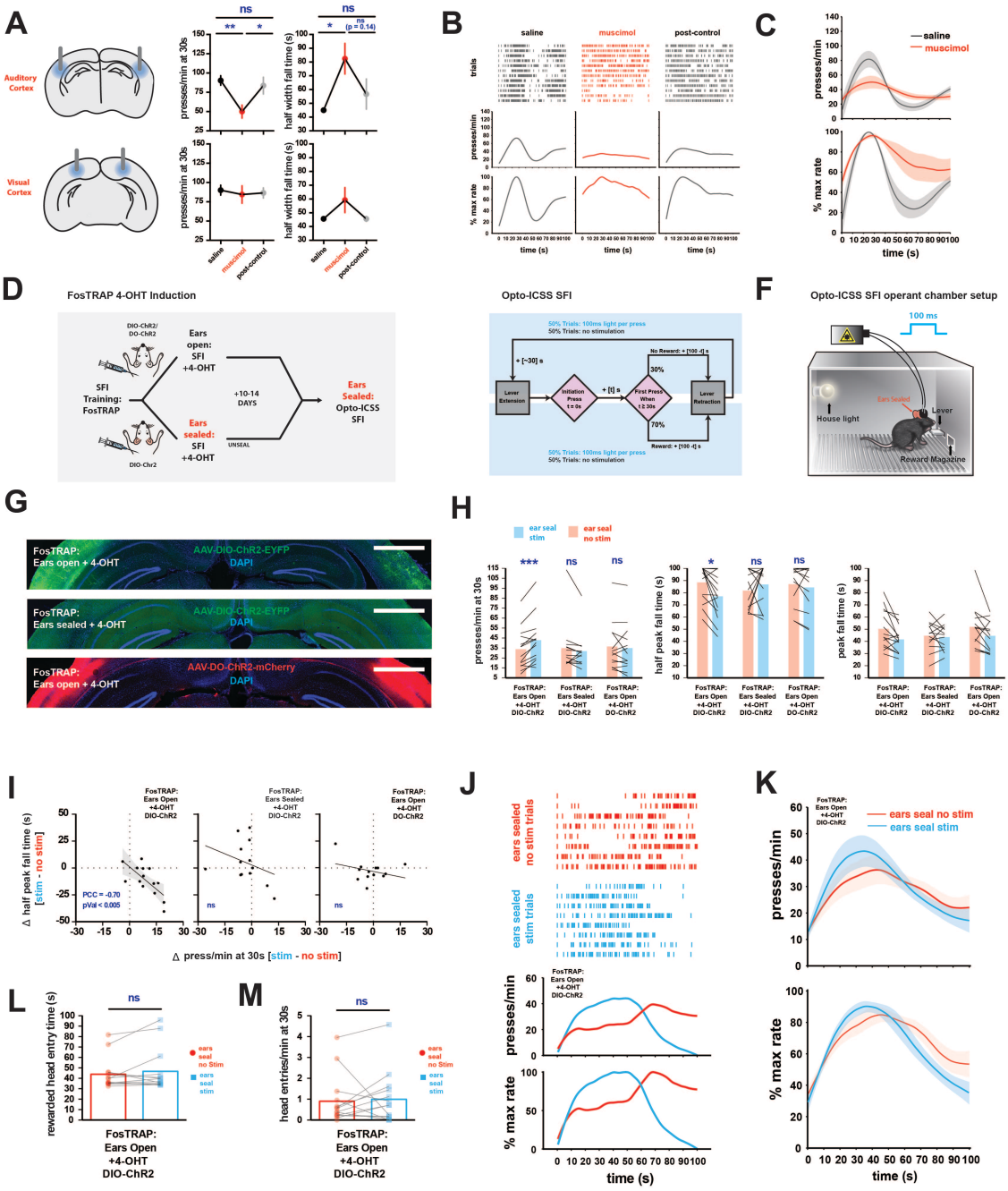
A
Auditory Cortex
Visual Cortex
presses/min at 30s
half width fall time (s)
ns
**
*
ns (p = 0.14)
saline
muscimol
post-control
B
saline
muscimol
post-control
trials
presses/min
% max rate
time (s)
C
saline
muscimol
presses/min
% max rate
time (s)
D
FosTRAP 4-OHT Induction
DIO-ChR2/ DO-ChR2
SFI Training: FosTRAP
Ears open: SFI +4-OHT
Ears sealed: SFI +4-OHT
+10-14 DAYS
UNSEAL
Ears Sealed: Opto-ICSS SFI
DIO-Chr2
Opto-ICSS SFI
50% Trials: 100ms light per press
50% Trials: no stimulation
+ [~30] s
Lever Extension
Initiation Press t = 0s
+ [5] s
First Press When t ≥ 30s
No Reward: + [100 -t] s
30%
70%
Lever Retraction
Reward: + [100 -t] s
F
Opto-ICSS SFI operant chamber setup
100 ms
House light
Ears Sealed
Lever
Reward Magazine
G
FosTRAP: Ears open + 4-OHT
AAV-DIO-ChR2-EYFP
DAPI
FosTRAP: Ears sealed + 4-OHT
AAV-DIO-ChR2-EYFP
DAPI
FosTRAP: Ears open + 4-OHT
AAV-DO-ChR2-mCherry
DAPI
H
ear seal stim
ear seal no stim
presses/min at 30s
half peak fall time (s)
peak fall time (s)
***
ns
*
FosTRAP: Ears Open +4-OHT DIO-ChR2
FosTRAP: Ears Sealed +4-OHT DIO-ChR2
FosTRAP: Ears Open +4-OHT DO-ChR2
I
Δ half peak fall time (s) [stim - no stim]
Δ press/min at 30s [stim - no stim]
PCC = -0.70
pVal < 0.005
ns
J
ears sealed no stim trials
ears sealed stim trials
presses/min
% max rate
time (s)
K
ears seal no stim
ears seal stim
presses/min
% max rate
time (s)
L
rewarded head entry time (s)
ns
ears seal no Stim
ears seal stim
FosTRAP: Ears Open +4-OHT DIO-ChR2
M
head entries/min at 30s
ns
ears seal no Stim
ears seal stim
FosTRAP: Ears Open +4-OHT DIO-ChR2

Figure 7. FosTRAP expression recapitulates cFos protein expression pattern in AuDd (A) FosTRAP animals were trained for 21 days on SFI and split into two groups. One group (top) was induced with 4-OHT after being injected with a Cre-dependent AAV expressing GFP and eventually sacrificed immediately after performing SFI again with ears open. The other group (bottom) performed the no lever version of the task also with ears open and immediately sacrificed following session completion. (B) Percent distribution across the cortical layers in AuDd of cFos protein and cFosCre (as visualized via Cre-dependent GFP expression) in FosTRAP animals (n = 4) that were induced (green) while performing SFI with their ears open and later in another SFI session immediately sacrificed upon completion (black), again with ears open. These distributions were compared to the cFos protein percent distribution of FosTRAP animals that were sacrificed upon completion of the no lever task (red) version with ears open (n = 4). Values are mean ± SEM. *$p < 0.05$; repeated measures-two-way ANOVA, Tukey's multiple comparisons. (C-E) AuDd cortical layer expression pattern of endogenous cFos protein for FosTRAP animals sacrificed immediately after performing SFI (C) and the no lever task version (D) with their ears open. (E) FosTRAP cFosCre expression as visualized via Cre-dependent GFP expression in AuDd of an animal induced with its ears open while performing SFI. Scale bar denotes 100 μm. D and L denote dorsal and lateral respectively.

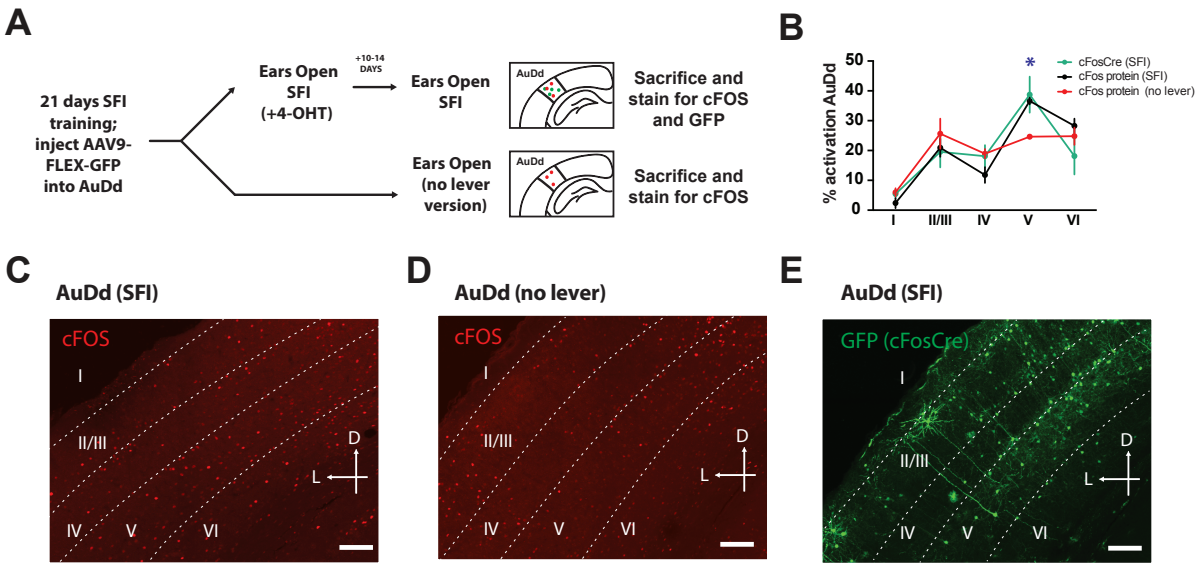
A
21 days SFI training; inject AAV9-FLEX-GFP into AuDd
Ears Open SFI (+4-OHT)
+10-14 DAYS
Ears Open SFI
AuDd
Sacrifice and stain for cFOS and GFP
Ears Open (no lever version)
AuDd
Sacrifice and stain for cFOS
B
% activation AuDd
50
40
30
20
10
0
I
II/III
IV
V
VI
*
cFosCre (SFI)
cFos protein (SFI)
cFos protein (no lever)
C
AuDd (SFI)
cFOS
I
II/III
IV
V
VI
D
L
D
AuDd (no lever)
cFOS
I
II/III
IV
V
VI
D
L
E
AuDd (SFI)
GFP (cFosCre)
I
II/III
IV
V
VI
D
L

Figure 8. Photoactivation of FosTRAPed, Cre-on cells via ChR2 in AuDd. (A) Single-units were recorded extracellularly from AuDd in FosTRAP animals (n = 2, 2 recording sessions) in which ChR2-eYFP was expressed in a Cre-on dependent manner following 4-OHT induction. (B) Raster plot (left) and PETH (right) of an example photo-tagged unit (significant response within 10 ms of light stimulus onset; $p<0.01$, Stimulus-Associated spike Latency Test (SALT). (C) Light modulation index (the difference in light-evoked and baseline FR divided by their sum) of all single-units recorded at different cortical depths. Filled dots indicate putatively photo-tagged units ($p < .01$, SALT). Bars indicate the mean light modulation index in 100 μm bins (unfilled: all units; filled photo-tagged units). Pie chart: percent of single-units that are putatively photo-tagged ($p<0.01$, SALT). (D) Single-units were recorded extracellularly from AuDd in FosTRAP animals (n = 2, 3 recording sessions) in which ChR2-mCherry was expressed in a Cre-off dependent manner following 4-OHT induction. (E-F) Same as B-C, but for Cre-off population.

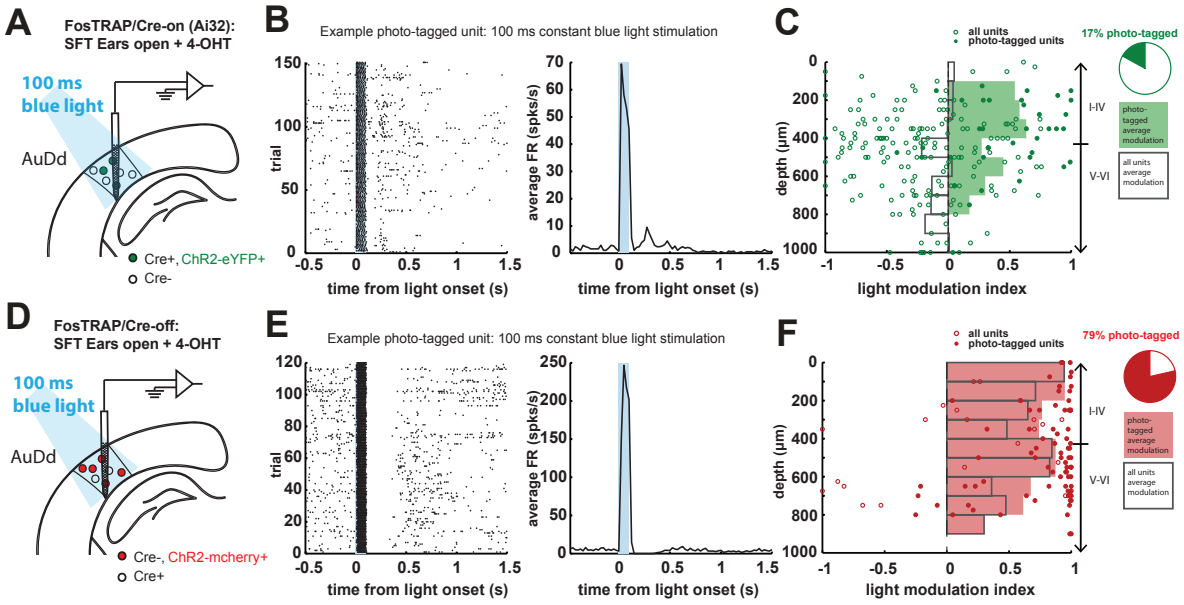
A
FosTRAP/Cre-on (Ai32):
SFT Ears open + 4-OHT
100 ms
blue light
AuDd
Cre+, ChR2-eYFP+
Cre-
B
Example photo-tagged unit: 100 ms constant blue light stimulation
trial
time from light onset (s)
average FR (spks/s)
time from light onset (s)
C
all units
photo-tagged units
17% photo-tagged
depth (µm)
I-IV
V-VI
photo-tagged average modulation
all units average modulation
light modulation index
D
FosTRAP/Cre-off:
SFT Ears open + 4-OHT
100 ms
blue light
AuDd
Cre-, ChR2-mcherry+
Cre+
E
Example photo-tagged unit: 100 ms constant blue light stimulation
trial
time from light onset (s)
average FR (spks/s)
time from light onset (s)
F
all units
photo-tagged units
79% photo-tagged
depth (µm)
I-IV
V-VI
photo-tagged average modulation
all units average modulation
light modulation index

Figure 9. AuDd layer V, striatal-projecting active population and SFI performance. (A) Strategy for labeling and manipulating layer V, striatal-projecting active populations in AuDd using rAAV2- ESARE-ERCreER-PEST. (B-C) ESARE expression patterns. Terminals in DMS (B) from ESARE populations in layer V of AuDd (C) expressing Cre-dependent ChR2/GFP. Scale bars denotes 100 μm. D and L denote dorsal and lateral respectively. (D) Opto-ICSS SFI response rates at 30s (left), half peak fall times (middle), and peak times (right) for optical stimulation and no stimulation omission trials under auditory deprivation using retrograde ESARE, activity-dependent labeling (n = 7). Bars are mean. * $p < 0.05$; paired t-tests. (E) Response rasters for stimulation and no stimulation trials (top), response rate PETHs (middle) and percent maximum response rate PETHs (bottom) of an exemplar stimulating layer V, ESARE, striatal-projecting populations in AuDd under auditory deprivation. (D) Stimulation and no stimulation average PETHs (n = 7) for response rate (top) and percent maximum response rate (bottom) for opto-ICSS SFI omission trials under auditory deprivation using retrograde, ESARE, activity-dependent labeling. Values are mean ± SEM. (F) Schematic representation of neural structures involved in sensorimotor feedback loop implicated in SFI timing behavior.

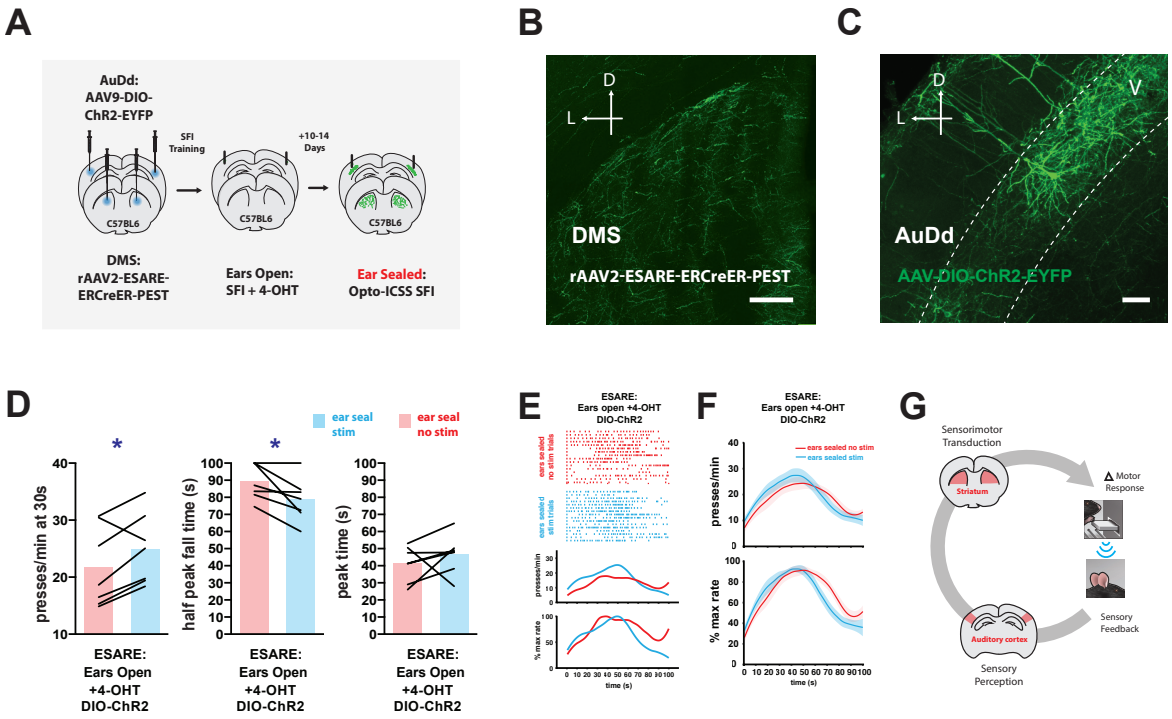
A
AuDd:
AAV9-DIO-
ChR2-EYFP
SFI
Training
+10-14
Days
C57BL6
C57BL6
C57BL6
DMS:
rAAV2-ESARE-
ERCreER-PEST
Ears Open:
SFI + 4-OHT
Ear Sealed:
Opto-ICSS SFI
B
D
L
DMS
rAAV2-ESARE-ERCreER-PEST
C
D
L
V
AuDd
AAV-DIO-ChR2-EYFP
D
ear seal stim
ear seal no stim
presses/min at 30s
half peak fall time (s)
peak time (s)
ESARE:
Ears Open
+4-OHT
DIO-ChR2
E
ESARE:
Ears open +4-OHT
DIO-ChR2
ears sealed no stim trials
ears sealed stim trials
presses/min
% max rate
time (s)
F
ESARE:
Ears open +4-OHT
DIO-ChR2
ears sealed no stim
ears sealed stim
presses/min
% max rate
time (s)
G
Sensorimotor
Transduction
Striatum
Motor
Response
Sensory
Feedback
Auditory cortex
Sensory
Perception

Chapter 6: Final conclusions

The self-initiated/terminated design of the task requires that animals maintain an internal representation of time in order to modulate their response rate. While the task design does not require repetitive responding to obtain a reward, animals develop an escalating response profile in anticipation of the learned reward time and, in the case of reward omission trials, a descending response profile upon realization that a reward will not appear (Figure 1). The acquisition of these rise and fall phases appears to be mutually dependent based on correlation analysis (Figure 2). The results from my work demonstrate that this repetitive, adjunctive pressing takes on an auxiliary capacity in overall timing performance, specifically via the sensory feedback derived from this type of action.

Timing literature to date has demonstrated that stereotyped, adjunctive action patterns under temporally-defined schedules of reinforcement appear to be related to an animal's subjective conception of time (Gouvêa et al., 2014), however, interpretation of these patterns is problematic. Adjunctive action patterns under timed reinforcement tend to be highly idiosyncratic with a wide range of behaviors (Haight and Killeen, 1991; Hodos et al., 2005; Laties et al., 1965; Machado and Keen, 2003; Skinner, 2004) emerging following training, marring the ability to discretely manipulate these patterns. The self-paced design of SFI primarily promotes the performance of a single action - pressing. Behavior in fixed-interval schedules of reinforcement is typically characterized by a delay in responding following trial initiation, with a bout of pressing that appears around the conditioned reinforcement time (Gibbon, 1977; Meck, 2006; Mello et al., 2015). This delay allows for animals to engage in other temporally mediating behaviors that cannot be tracked or manipulated. In contrast, animals performing SFI show a continual engagement with the lever from trial initiation, most likely due

to the design of SFI requiring the animal to initiate the fixed-interval, rather than initiation being signaled by an external cue. The sensory deprivation experiments and associated controls demonstrate that animals utilize the sound derived from pressing to help shape peak dynamics (Figures 3 and 4). The results point toward the role of a potential sensorimotor feedback loop in a self-paced, motor timing task, where changes in action state could be inferred from the sensory consequences of an ongoing adjunctive cue.

Interestingly, the auditory system has been extensively implicated in timing. Literature has demonstrated the dominance of this modality in conveying temporal information about repetitive movement (Nobre and van Ede, 2018; Pizzera and Hohmann, 2015; Repp and Penel, 2002; 2003; Welch et al., 1986). Furthermore, neurons in the auditory cortex have been shown to be sensitive to stimuli durations (Brosch and Schreiner, 1997; Brosch et al., 2011; He et al., 1997; Zhou et al., 2010). At a neuronal level this tuning is too small to account for the perception of durations in the 10s of seconds. However, state-dependent network models of the cortex, incorporating short-term plasticity and inhibitory post-synaptic potentials that operate in the context of an incoming sensory input (i.e. conveying state) can explain tuning for complex temporal stimuli of longer durations (Buonomano and Merzenich, 1995; Buonomano and Maass, 2009). The results from my work demonstrate that active populations in the auditory cortex, activated by the sound of repetitive lever pressing (Figure 5) can partially rescue timing dynamics under sensory deprivation following training (Figure 6). Importantly, the observed rescue effects from auditory cortex press-dependent stimulation do not result in generalized increases in responding across the entire probe trial, but an increase in responding at 30s paired with a decrease in half peak fall times (i.e. an improvement in timing dynamics; Figure 6I) implicating this feedback mechanism in the calculus of timing. While pressing and auditory

feedback appear to be the default sensorimotor mechanism in SFI, it is possible that temporally mediating adjunctive behaviors could be processed by a different sensory modality under other time-based reinforcement schedules that promote different task performance features.

My results also show that layer V cortical activation appears to be specifically blocked under sensory deprivation (Figure 5E) and in a task version where no lever is present (Figures 7B). Layer V projections from the auditory cortex to the striatum are known to mediate auditory-based action selection (Znamenskiy and Zador, 2013) and medium spiny neurons have been shown to modulate the response dynamics in fixed-interval tasks (Drew et al., 2007; Ward et al., 2009). Furthermore, spatiotemporal firing patterns have been observed in the striatum with fixed-interval learning that reflect timing behavior (Jin et al., 2009; Mello et al., 2015). A recent timing model has described excitatory, cortical input as molding this spatiotemporal pattern in the striatum through training, scaling the recurrent population responses to the target interval (Murray and Escola, 2017). By parsing out striatal-projecting active populations in the auditory cortex through retro-labeling, I have implicated the striatum as a potential motor output pathway for the online transduction of self-derived auditory cues from adjunctive responding, whereby motor responses can be fine tuned and modified with respect to time (Figure 9).

In the songbird auditory system, feedback mechanisms (Margoliash, 1983; McCasland and Konishi, 1981; Sakata and Brainard, 2008) believed to be involved in online modulation of syllable timing (Sakata and Brainard, 2006) have been observed in the posterior descending pathway. Within this circuit, the high vocal center (HVC), a sensory-motor nucleus in the avian brain, has been shown to exhibit a sparse firing code that drives the robust nucleus of the arcopallium, a downstream motor nucleus, at specific time points during song production (Hahnloser et al., 2002). The HVC is sensitive to perturbations in auditory feedback (Sakata and

Brainard, 2008) and cooling of this nucleus slows song speed while keeping song structure intact (Long and Fee, 2008), implicating it in motor timing. Deafening experiments and recordings in HVC have demonstrated that control over syllable repetition counts in song may be dependent on an adapting, auditory-motor, positive feedback loop in the posterior descending pathway (Wittenbach et al., 2015). Thus, in the songbird, auditory feedback might help to sustain repetitions as well as to stop them from continuing for too long. My results, implicate a similar mechanism for self-paced timing in the mammalian brain. I have identified active populations in the auditory cortex that are modulated by action and also capable of reciprocally modulating future action (Figure 9F). Feedback from a repetitive, action-derived sound drives increases in responding over a target time range (~30 s) and decaying response rates at later times (~70 s).

It is important to note that I am not claiming sensorimotor feedback is singularly responsible for how timed motor responses are produced, but could exist in parallel with other timing mechanisms. Animals are still able to press under sensory deprivation, but show lower response rates and poorer timing dynamics, indicating pressing is not entirely sensory feedback dependent (Figure 3C). These effects appear to titrate with the amount of auditory input (Figure 5B), as observed in the unilateral ear sealing experiments, suggesting that sensory feedback plays an online, modulatory role in the motor response profile. It has become increasingly apparent for the need to draw distinctions in the type of timing being tested, with motor and sensory timing being the two broad classifications of task designs (Meck and Ivry, 2016; Paton and Buonomano, 2018). Within this classification system, SFI would be considered classically motor in nature, since it requires animals to produce a precise action pattern over time. This is in contrast to paradigms such as an interval discrimination task, in which animals have to gauge a sensory event as shorter or longer relative to some standard. Interestingly, the results from my research

demonstrate an unexpected sensory performance feature of SFI that is independent of reward related cues and dependent on action.

As previously mentioned, motor-based timing models have described population networks (Goldman, 2009; Laje and Buonomano, 2013; Liu and Buonomano, 2009; Miller and Jin, 2013), such as those observed in the striatum, that appear with learning and can tell time through their spatiotemporal firing patterns (Jin et al., 2009; Mello et al., 2015). It has also been demonstrated that cortical circuits seem to be necessary for the learning of motor sequences, but redundant once behavior is fully acquired (Kawai et al., 2015), at which point subcortical circuits supposedly become self-autonomous in performing motor timing (Murray and Escola, 2017). In contrast, models of sensory timing (Buonomano and Merzenich, 1995; Buonomano and Maass, 2009), such as state-dependent models, require continual sensory input processed via cortical circuits to explain how the system can gauge the passage of time, and as such cannot explain the production of anticipatory motor behavior. An interesting hypothesis is that SFI promotes a hybrid approach to dealing with timing. Indeed, my data demonstrate a role for modal cortical activation and striatal projections even once timing behavior is fully acquired (Figure 6 and 9). One possibility is that the self-paced design of the task promotes a unique intersection of sensory and motor task features, whereby cortical activation, driven by a repetitive self-generated sensory cue, is necessary even once motor timing behavior is fully learned. Modifying timing task designs to promote motor and/or sensory features could prove to be a lucrative line of future investigations regarding how timing mechanisms emerge in the brain. Nevertheless, the results presented in this dissertation add to a growing body of literature, which demonstrates the degree to which our representation of time is enriched and altered by sensory experience (Ahrens and Sahani, 2011; Ortega and López, 2008; Pariyadath and Eagleman, 2007; Stetson et al., 2006).

Uniquely, this data demonstrates a previously unappreciated aspect of this sensory experience in complex motor timing – action self-monitoring.

Parts of chapter 6 are currently in preparation for submission for publication (Jonathan Cook, Bella Nguyen, Payaam Mahdavian, Megan Kirchgessner, Patrick Strassmann, Max Engelhardt, Edward M. Callaway, and Xin Jin). The dissertation author was the primary researcher and author of this material.

Appendix: Methods

A.1 Experimental subjects

All procedures were approved by the Institutional Animal Care and Use Committee at the Salk Institute for Biological Studies, and were conducted in accordance with the National Institute of Health's Guide for the Care and Use of Laboratory Animals. Adult C57BL/6J and FosTRAP (Jackson laboratory, stock no: 021882; Guenthner et al., 2013) male and female mice were group housed on a reverse light cycle with ad libitum access to food and water. Operant training began at 8 weeks of age. Animals were food deprived for 48 hours to reach roughly 85% of their initial body weight and then underwent three days of a continuous reinforcement schedule before starting the SFI training schedule (see below under Behavioral training and analysis; (Howard et al., 2017).

A.2 Behavioral training and analysis

Animals were trained in a modular operant chamber (Med Associates Inc.) fitted with ultrasensitive, retractable levers to the left of the reward magazine. The reward magazine was fitted with an infrared beam break sensor to monitor head entries. Following food deprivation, animals underwent three days on a continuous reinforcement training schedule (15 reinforcements per day) in which responding on the lever to the left of the reward magazine yielded a 20 mg, nutritionally balanced pellet (BioServ). Following continuous reinforcement training, animals were trained for 21 days on the self-paced fixed-interval (SFI) 30s schedule (50 reinforcements per day – see Figure 1A and main text for specifics of schedule design) again utilizing the lever to the left of the reward magazine and 20 mg pellets for reinforcement. In addition to 50 reinforcement pellets daily, animals received 1.5-2.5 g rodent chow per day to prevent body weight from dropping below 85% of initial body weight. The exact amount of

chow provided each day was adjusted to keep deprivation weight stable. Reinforcement training schedules were written using MED-PC programming language and behavioral data was analyzed offline using custom scripts written in Matlab. The half peak fall time was calculated using the intersection point of the response rate PETH with the line y = 50% maximum response rate. The response rate PETH was constructed using a moving average function with a smoothing window of 15 s - the minimum duration found to provide the least noise yielding a single half peak fall time value. Peak values were calculated using the midpoint of the two intersection points of the response rate PETH with the line y = 85% maximum response rate. For acute sensory deprivation and pharmacological/optogenetic experiments, a performance criterion was used to exclude animals that showed poor peak dynamics on the day prior to experimental manipulation. Animals' half peak fall times asymptote with training indicating stable peak formation behavior (Figure 1F; day 21: mean = 46.17 s, standard deviation = 3.63 s). To ensure that animals properly learned peak timing behavior before being tested on sensory deprivation and pharmacological/optogenetic experiments, individuals that showed half peak fall times greater than 50 s (mean + standard deviation) were excluded from manipulation results.

A.3 Three-day acute sensory experiments

The week following training on the SFI schedule, animals underwent three-day acute sensory manipulations (cutaneous/proprioceptive, visual and auditory) performing the same task. Cutaneous/proprioceptive sensory deprivation was achieved via a forelimb nerve block (Koch et al., 2017), in which 50 ul of a lidocaine cocktail (0.5% lidocaine, 10mM CNQX in 0.9 % sterile saline) was injected on the internal side of the pectoral girdle of the left and right forelimb. The injected volume was adjusted such that animals could still press the lever, but exhibited no withdrawal reflex to pinching the forepaw toes. Animals received 0.9 % saline injections in the

same locations on the pre-control day and no treatment on the post-control day. For visual deprivation, the house light was turned off on the manipulation day and on in the pre and post-control days. Finally, for auditory deprivation, a small amount of cotton was placed inside the ear cavity and the ear canal reversibly sealed using a small amount of vet bond. For pre-control and post-control days, animals had their ears open. Auditory and cutaneous/proprioceptive sensory manipulations were performed under 3-4% isoflurane anesthesia 15-20 minutes before beginning behavior. For auditory deprivation experiments, Vetbond was removed using ethanol, also under isoflurane, and ears were monitored post-procedurally for treatment of inflammation by veterinarian staff. The sensory experiments were performed to specifically test the effect of omitting specific sensory modalities on the performance of SFI. However, it was found that under auditory deprivation, reward retrieval time also changed. Delays in reward retrieval time can alter animals' timing performance and consequently prevent an accurate interpretation of the manipulation results in isolation. A criterion of the minimum change in reward retrieval time allowed across the pre-control day and manipulation days was imposed to prevent animals from learning a new reward retrieval time on the manipulation day. Across the pre and post-control days for the ear sealing experiments, animals show a skewed distribution of reward retrieval time changes (pre-control vs. post-control; Δ reward retrieval time: median = 0.72 s, standard deviation = 2.31 s). To reduce the impact of any changes in pellet retrieval time, animals that exhibited changes in reward retrieval time greater than 5 seconds (median + 2*standard deviation) compared to the pre-control day were omitted from the experimental groups.

A.4 Activity-dependent labeling

To label active populations with CreERT^2, FosTRAP animals (Guenthner et al., 2013) were given 4-OHT on day 21 of SFI training. 4-OHT is a metabolized version of tamoxifen and

as such allows for a narrower temporal window over which activity-dependent labeling can take place. It has been previously demonstrated in the visual cortex that maximum labeling occurs when sensory input is provided an hour before injection of 4-OHT, with minimal to no labeling occurring around 5-6 hours before and after injection (Guenthner et al., 2013). For the day of labeling, animals with their ears sealed bilaterally or open were placed in the operant chamber an hour before SFI was initialized. Furthermore, they were run on an extended SFI schedule in which they received 100 reward pellets. As in regular SFI training, rewarded trials occurred 70% of time and probe trials occurred 30% of the time. Animals received a dose of 50 mg per kg 4-OHT in chen oil after receiving roughly 50 rewards. Following completion of 100 rewards animals were left in the chamber for an additional hour before being returned to their home cage. To acclimate animals to the disruption of receiving an intraperitoneal injection during SFI performance, animals received saline injections upon completion of the first 20 rewards in the week leading up to induction day. For the striatal-projecting experiments using rAAV2-ESARE-ERCreER-PEST (Kawashima et al., 2013), C57BL/6J mice had stereotaxic injections and implants performed prior to training and were induced in the same way as FosTRAP animals on day 21 of training.

A.5 Stereotaxic surgery

Prior to training on SFTSFI, mice were administered a xylazine and ketamine cocktail (10 mg per kg and 100 mg per kg, respectively) intraperitoneally and placed inside a stereotaxic surgical frame (Kopf). Craniotomies were made using a drill (Drummond). For optogenetic experiments targeting the auditory cortex, 1μl concentrated AAV (University of Pennsylvania Vector Core AAV9-DIO-ChR2-EYFP; Salk Institute Vector Core AAV9-DO-ChR2-mCherry) was bilaterally injected using a manual syringe (Hamilton) into the following coordinates: -2.3

AP, ±4.0 ML, -0.66 DV. Following viral injections, custom-made optrodes consisting of a ceramic ferrule and fiber optic cable (200 um, Thor Labs) were lowered into the brain slightly above the auditory cortex injection site (-2.3 AP, ±4.0 ML, -0.65 DV)(Howard et al., 2017). The optrodes were affixed to the skull using optibond (Kerr 35129) and light activated dental cement (Ivoclar Viviadent 595953WW). For the striatal-projecting experiments, C57BL/6J animals were injected with the 0.3 μl of rAAV2-ESARE-ERCreER-PEST (Salk Institute Vector Core) or rAAV2-Cre (Salk Institute Vector Core) in the dorsal striatum (+0.34 AP, ±2.25 ML, -2.30 DV). For cannula implantation (see below under Three-day muscimol experiments), mice had guide cannulas (Plastics One C313GS-4/SPC) affixed to the skull targeting the same location of the auditory cortex as with optrode implantation. Following all surgical procedures, mice received analgesia consisting of buprenorphine (1 mg per kg) and were allowed to recover for one week before beginning training on SFTSFI.

A.6 Three-day muscimol experiments

Following 21 days of training on SFTSFI and then recovery from cannula implantation surgery, C57BL/6J animals were retrained on SFTSFI before undergoing a three-day pharmacological manipulation experiment. As with the sensory experiments, the manipulation day in which muscimol was infused was flanked by two control days in which no pharmacological manipulation occurred. Dummy cannulas (Plastics One C313DCS-4/SPC) cut to be flush with the end of the guide cannula remained inserted during all times, apart from infusions, to prevent debris from entering the brain. For the pre-control day, animals received a bilateral infusion of 0.5 μl saline delivered at flow rate of 0.5 μl per minute, 30 minutes before starting SFTSFI. For the post-control day, no infusions were performed. On the manipulation day, animals received 0.5 μl of 1.0 μg/μl muscimol in saline delivered bilaterally at a flow rate

0.5 μl per minute, 30 minutes before starting SFTSFI (Geddes et al., 2018). This flow rate and concentration results in the delivery of 0.5 μg of muscimol, which has been demonstrated to result in 90% tissue inactivation 1-3 mm^3 from the site of infusion (Lewis and Gould, 2007). Muscimol and saline were infused via an infusion cannula (Plastics One C313IS-4/SPC) that was cut to protrude 0.5 mm beyond the base of the guide cannula. For all infusions, animals were physically restrained and infusion cannulas were left in place for 5 minutes following the completion of infusion before being removed and the dummy cannulas returned. Infusion cannulas were attached to 28-gauge polyethylene tubing (Plastics One PE50). The tubing was attached to 1 ml syringes (BASi MDN-0100) being depressed by flow rate controllable microinfusion pump system (BASi MD-1000, MD-1001, MD-1002).

A.7 Behavioral optogenetic experiments

Following 21 days of SFI training and surgery, implanted animals were retrained for one week on SFI before undergoing a single optical stimulation experiment occurring between 12-14 days post surgery. For retraining and stimulation, animals were tethered via fiber optic cables connecting optrode ferrules to a commutator. On the day of optogenetic stimulation, animals had their ears sealed and received 100 ms constant blue light stimulation (Laserglow 473 nm, 5mW) with each lever press(Howard et al., 2017). Optical stimulation occurred whenever the lever was pressed and was not restricted to any time window over probe or rewarded trials. The MED-PC software randomly selected stimulation trials for 50% of the rewarded trials and 50% of the probe trials (Howard et al., 2017). For a normal SFI training session animals perform 50 rewarded trials, with probe trials occurring 30% of time and rewarded trials occurring 70% of time. To ensure there were enough stimulated and non-stimulated probe trials, animals were allowed to perform 100 rewarded trials for the day of optical stimulation.

A.8 Electrophysiological experiments

At least one day prior to recording, animals were implanted with a headframe while under anesthesia with isoflurane. A circle of skin, approximately 10mm in diameter was removed to make room for the headframe implant. The skull was cleaned and headframe implant was secured with Vetbond (Santa Cruz Biotechnology sc-361931) and Metabond (Parkell S380). The headframe was placed as centrally as possible with right-hemisphere AuDd still accessible within the inner well of the headframe. For all animals, the inner well of the headframe implant was filled with Kwik-Cast sealant (WPI KWIK-CAST) until recording. Electrophysiological recordings were performed in the right hemisphere AuDd of one 4-OHT/open/on animal (2 penetrations) and two 4-OHT/open/off animals (3 total penetrations). Under 2% isoflurane anesthesia, a small craniotomy was made over AuDd and filled with ACSF. Subsequently, the animals were removed from anesthesia and head-fixed on a custom-made wheel. Under this set-up animals were free to run at will. A 64-channel silicon microprobe (Du et al., 2011), with channels spanning 1.05 mm, was lowered into the craniotomy. An optical fiber (1mm diameter, .39 NA, Thor Labs) was positioned as close as possible to the craniotomy without touching the probe for optical stimulation. LED stimulation via a blue LED driver (T-Cube, 470nm, Thor Labs) was controlled by Arduino. Trials consisted of a 500ms prestimulus period (used for determining baseline firing rate) and 100ms constant, 8-10 mW LED stimulation with 2-4 second inter-stimulus intervals. Spikes were extracted and sorted into clusters using Kilosort (Stringer et al., 2016) followed by manual cleaning and verification (Phy Template-Gui: https://github.com/kwikteam/phy/blob/master/ README.md). All single-units with <1% refractory period violations and waveform amplitudes at least two standard deviations above the noise were included for subsequent analyses (Howard et al., 2017).

A.9 Histological processing and stereological analysis

Mice were administered a xylazine and ketamine cocktail (10 mg per kg and 100 mg per kg, respectively) intraperitoneally and transcardially perfused with 8-10 ml of 0.9% saline, followed by 8-10 ml of 4% paraformaldehyde in PBS. Following extraction, brains were placed in 4% paraformaldehyde in PBS overnight, before being placed in 30% sucrose in PBS for 5-7 days in preparation for sectioning. 40 μm coronal sections were prepared using a freezing microtome and tissue was labeled with the following antibodies: chicken anti-GFP (1:500; Aves Labs GFP-1020), mouse anti-mCherry (1:500; Clontech 632543), rabbit anti-cFos (1:500; Synaptic Systems 226 003), alexa-488 donkey anti-chicken (1:250; Jackson Immuno Research 703-545-155), Cy3 donkey anti-rabbit (1:250; Jackson Immuno Research 711-165-152) and Cy3 donkey anti-mouse (1:250; Jackson Immuno Research 715-165-151). For secondary and primary incubations, antibody blocking was performed using normal horse serum (Sigma-Aldrich H0146). Antibody amplification was used to visualize ChR2-mCherry and ChR2-EYFP. Images were taken at x20 using an Olympus VS120 slide scanner (Howard et al., 2017).

A.10 cFos cell counting

Following 21 days of training on SFI, C57BL6 animals each had a single ear randomly sealed and were then allowed to perform a full session of SFI. At the completion of the session animals were immediately sacrificed. Prior to sectioning, brains were scored with a line across the cortex of the left hemisphere to ensure counts for a given hemisphere were correctly associated with the sealed or open ear. Images taken with the VS120 slide scanner were saved as JPEG files using the Olympus offline proprietary software, VS-ASW. Images were then overlayed in Adobe Photoshop with coronal section maps from the mouse Allen brain atlas (mouse.brain-map.org) and manually counted (Klug et al., 2018).

A.11 Statistical analyses

Learning performance, sensory deprivation experiments, pharmacological/optogenetic manipulations, and cFos expression experiments were analyzed using one-way repeated-measures ANOVA with post-hoc multiple comparison tests. Extinction effects and experiments testing the role of the percentage of probe trials on performance were analyzed using an unpaired t-test. Analyses of the rewarded head entry time and head entry rate for the 4-OHT/open/on group were analyzed using a paired t-test. Statistical analyses were done using MATLAB and Prism software.

A.12 Author contributions

Jonathan Cook and Xin Jin designed the research. Jonathan Cook, Bella Nguyen, and Payaam Mahdavian performed behavioral training and behavioral manipulation experiments (sensory deprivation, muscimol inactivation and optical stimulation). Jonathan Cook and Bella Nguyen performed stereotaxic surgeries. Jonathan Cook and Bella Nguyen performed perfusions, histology and immunohistochemistry. Jonathan Cook performed microscopy. Jonathan Cook, Payaam Mahdavian and Max Engelhardt performed cell counting. Jonathan Cook analyzed behavioral (sensory deprivation, muscimol inactivation and optical stimulation) and immunohistochemical data. Megan Kirchgessner performed electrophysiological experiments and associated analyses. Jonathan Cook constructed the figures.

Parts of this appendix are currently in preparation for submission for publication (Jonathan Cook, Bella Nguyen, Payaam Mahdavian, Megan Kirchgessner, Patrick Strassmann, Max Engelhardt, Edward M. Callaway, and Xin Jin). The dissertation author was the primary researcher and author of this material.

Bibliography

Ahrens, M.B., and Sahani, M. (2011). Observers Exploit Stochastic Models of Sensory Change to Help Judge the Passage of Time. Current Biology *21*, 200–206.

Brosch, M., and Schreiner, C.E. (1997). Time course of forward masking tuning curves in cat primary auditory cortex. Journal of Neurophysiology *77*, 923–943.

Brosch, M., Selezneva, E., and Scheich, H. (2011). Formation of associations in auditory cortex by slow changes of tonic firing. Hearing Research *271*, 66–73.

Buonomano, D.V. (2000). Decoding temporal information: A model based on short-term synaptic plasticity. J. Neurosci. *20*, 1129–1141.

Buonomano, D.V., and Merzenich, M.M. (1995). Temporal information transformed into a spatial code by a neural network with realistic properties. Science *267*, 1028–1030.

Buonomano, D.V., and Maass, W. (2009). State-dependent computations: spatiotemporal processing in cortical networks. Nat Rev Neurosci *10*, 113–125.

Crawley, J.N., Belknap, J.K., Collins, A., Crabbe, J.C., Frankel, W., Henderson, N., Hitzemann, R.J., Maxson, S.C., Miner, L.L., Silva, A.J., et al. (1997). Behavioral phenotypes of inbred mouse strains: implications and recommendations for molecular studies. Psychopharmacology *132*, 107–124.

Drew, M.R., Simpson, E.H., Kellendonk, C., Herzberg, W.G., Lipatova, O., Fairhurst, S., Kandel, E.R., Malapani, C., and Balsam, P.D. (2007). Transient Overexpression of Striatal D2 Receptors Impairs Operant Motivation and Interval Timing. Journal of Neuroscience *27*, 7731–7739.

Du, J., Blanche, T.J., Harrison, R.R., Lester, H.A., and Masmanidis, S.C. (2011). Multiplexed, high density electrophysiology with nanofabricated neural probes. PLoS ONE *6*, e26204.

Eagleman, D.M. (2008). Human time perception and its illusions. Current Opinion in Neurobiology *18*, 131–136.

Eliades, S.J., and Wang, X. (2008). Neural substrates of vocalization feedback monitoring in primate auditory cortex. Nature *453*, 1102–1106.

Falk, J.L. (1971). The nature and determinants of adjunctive behavior. Physiology and Behavior *6*, 577–588.

Geddes, C.E., Li, H., and Jin, X. (2018). Optogenetic Editing Reveals the Hierarchical Organization of Learned Action Sequences. Cell *174*, 32–43.e15.

Gibbon, J. (1977). Scalar expectancy theory and Weber's law in animal timing. Psychological Review *84*, 279–325.

Goldman, M.S. (2009). Memory without feedback in a neural network. Neuron *61*, 621–634.

Gouvêa, T.S., Monteiro, T., Soares, S., Atallah, B.V., and Paton, J.J. (2014). Ongoing behavior predicts perceptual report of interval duration. Front Neurorobiot *8*, 1–9.

Guenthner, C.J., Miyamichi, K., Yang, H.H., Heller, H.C., and Luo, L. (2013). Permanent Genetic Accessto Transiently Active Neurons via TRAP: Targeted Recombination in Active Populations. Neuron *78*, 773–784.

Hahnloser, R.H.R., Kozhevnikov, A.A., and Fee, M.S. (2002). An ultra-sparse code underlies the generation of neural sequences in a songbird. Nature *419*, 65–70.

Haight, P.A., and Killeen, P.R. (1991). Adjunctive behavior in multiple schedules of reinforcement. Animal Learning and Behavior *19*, 257–263.

He, J., Hashikawa, T., Ojima, H., and Kinouchi, Y. (1997). Temporal integration and duration tuning in the dorsal zone of cat auditory cortex. Journal of Neuroscience *17*, 2615–2625.

Hodos, W., Ross, G.S., and Brady, J.V. (2005). Complex response patterns during temporally spaced responding. Journal of the Experimental Analysis of Behavior *5*, 473–479.

Howard, C.D., Li, H., Geddes, C.E., and Jin, X. (2017). Dynamic Nigrostriatal Dopamine Biases Action Selection. Neuron *93*, 1436–1450.e1438.

Jin, D.Z., Fujii, N., and Graybiel, A.M. (2009). Neural representation of time in cortico-basal ganglia circuits. PNAS *106*, 19156–19161.

Kawai, R., Markman, T., Poddar, R., Ko, R., Fantana, A.L., Dhawale, A.K., Kampff, A.R., and Ölveczky, B.P. (2015). Motor Cortex Is Required for Learning but Not for Executing a Motor Skill. Neuron *86*, 800–812.

Kawashima, T., Kitamura, K., Suzuki, K., Nonaka, M., Kamijo, S., Takemoto-Kimura, S., Kano, M., Okuno, H., Ohki, K., and Bito, H. (2013). Functional labeling of neurons and their projections using the synthetic activity–dependent promoter E-SARE. Nat Meth *10*, 889–895.

Killeen, P.R., and Fetterman, J.G. (1988). A Behavioral Theory of Timing. Psychological Review *95*, 274–295.

Klug, J.R., Engelhardt, M.D., Cadman, C.N., Li, H., Smith, J.B., Ayala, S., Williams, E.W., Hoffman, H., and Jin, X. (2018). Differential inputs to striatal cholinergic and parvalbumin interneurons imply functional distinctions. eLife *7*, 47.

Koch, S.C., Del Barrio, M.G., Dalet, A., Gatto, G., Günther, T., Zhang, J., Seidler, B., Saur, D., Schüle, R., and Goulding, M. (2017). RORβ Spinal Interneurons Gate Sensory Transmission during Locomotion to Secure a Fluid Walking Gait. Neuron *96*, 1419–1431.e5.

Kvitsiani, D., Ranade, S., Hangya, B., Taniguchi, H., Huang, J.Z., and Kepecs, A. (2013). Distinct behavioural and network correlates of two interneuron types in prefrontal cortex. Nature

498, 363–366.

Laje, R., and Buonomano, D.V. (2013). Robust timing and motor patterns by taming chaos in recurrent neural networks. Nature Neuroscience *16*, 925–933.

Laties, V.G., Weiss, B., Clark, R.L., and Reynolds, M.D. (1965). Overt "mediating" behavior during temporally spaced responding. Journal of the Experimental Analysis of Behavior *8*, 107–116.

Lewis, M.C., and Gould, T.J. (2007). Reversible inactivation of the entorhinal cortex disrupts the establishment and expression of latent inhibition of cued fear conditioning in C57BL/6 mice. Hippocampus *17*, 462–470.

Liu, J.K., and Buonomano, D.V. (2009). Embedding multiple trajectories in simulated recurrent neural networks in a self-organizing manner. J. Neurosci. *29*, 13172–13181.

Long, M.A., and Fee, M.S. (2008). Using temperature to analyse temporal dynamics in the songbird motor pathway. Nature *456*, 189–194.

Machado, A. (1997). Learning the temporal dynamics of behavior. Psychological Review *104*, 241–265.

Machado, A., and Keen, R. (2003). Temporal discrimination in a long operant chamber. Behavioural Processes *62*, 157–182.

Malapani, C., Rakitin, B., Levy, R., Meck, W.H., Deweer, B., Dubois, B., and Gibbon, J. (1998). Coupled Temporal Memories in Parkinson's Disease: A Dopamine-Related Dysfunction. Journal of Cognitive Neuroscience *10*, 316–331.

Margoliash, D. (1983). Acoustic parameters underlying the responses of song-specific neurons in the white-crowned sparrow. Journal of Neuroscience *3*, 1039–1057.

Matell, M.S., and Meck, W.H. (2004). Cortico-striatal circuits and interval timing: coincidence detection of oscillatory processes. Cognitive Brain Research *21*, 139–170.

Matell, M.S., Meck, W.H., and Nicolelis, M.A.L. (2003). Interval timing and the encoding of signal duration by ensembles of cortical and striatal neurons. Behavioral Neuroscience *117*, 760–773.

McCasland, J.S., and Konishi, M. (1981). Interaction between auditory and motor activities in an avian song control nucleus. PNAS *78*, 7815–7819.

Meck, W.H. (2006). Neuroanatomical localization of an internal clock: A functional link between mesolimbic, nigrostriatal, and mesocortical dopaminergic systems. Brain Research *1109*, 93–107.

Meck, W.H., and Ivry, R.B. (2016). Editorial overview: Time in perception and action. Current Opinion in Behavioral Sciences *8*, vi–x.

Meck, W.H., Penney, T.B., and Pouthas, V. (2008). Cortico-striatal representation of time in animals and humans. Current Opinion in Neurobiology *18*, 145–152.

Mello, G.B.M., Soares, S., and Paton, J.J. (2015). A Scalable Population Code for Time in the Striatum. Current Biology *25*, 1113–1122.

Miller, A., and Jin, D.Z. (2013). Potentiation decay of synapses and length distributions of synfire chains self-organized in recurrent neural networks. Phys Rev E Stat Nonlin Soft Matter Phys. *88*, 062716.

Mita, A., Mushiake, H., Shima, K., Matsuzaka, Y., and Tanji, J. (2009). Interval time coding by neurons in the presupplementary and supplementary motor areas. Nature Neuroscience *12*, 502–507.

Murakami, M., Vicente, M.I., Costa, G.M., and Mainen, Z.F. (2014). Neural antecedents of self-initiated actions in secondary motor cortex. Nature Neuroscience *17*, 1574–1582.

Murray, J.M., and Escola, G.S. (2017). Learning multiple variable-speed sequences in striatum via cortical tutoring. eLife *6*, e26084–24.

Namboodiri, V.M.K., Huertas, M.A., Monk, K.J., Shouval, H.Z., and Shuler, M.G.H. (2015). Visually Cued Action Timing in the Primary Visual Cortex. Neuron *86*, 319–330.

Nobre, A.C., and Van Ede, F. (2018). Anticipated moments: temporal structure in attention. Nat Rev Neurosci *19*, 34–48.

Ortega, L., and López, F. (2008). Effects of visual flicker on subjective time in a temporal bisection task. Behavioural Processes *78*, 380–386.

Otazu, G.H., Tai, L.-H., Yang, Y., and Zador, A.M. (2009). Engaging in an auditory task suppresses responses in auditory cortex. Nature Neuroscience *12*, 646–654.

Pariyadath, V., and Eagleman, D. (2007). The effect of predictability on subjective duration. PLoS ONE *2*, e1264.

Paton, J.J., and Buonomano, D.V. (2018). The Neural Basis of Timing: Distributed Mechanisms for Diverse Functions. Neuron *98*, 687–705.

Peters, A.J., Chen, S.X., and Komiyama, T. (2014). Emergence of reproducible spatiotemporal activity during motor learning. Nature *510*, 263–267.

Pizzera, A., and Hohmann, T. (2015). Acoustic Information During Motor Control and Action Perception: A Review. The Open Psychology Journal *8,* 183-191.

Repp, B.H., and Penel, A. (2002). Auditory Dominance in Temporal Processing: New Evidence From Synchronization With Simultaneous Visual and Auditory Sequences. Journal of Experimental Psychology: Animal Behavior Processes *28*, 1085–1099.

Repp, B., and Penel, A. (2003). Rhythmic movement is attracted more strongly to auditory than to visual rhythms. Psychological Research *68*, 252–270.

Roberts, S. (1981). Isolation of an internal clock. Journal of Experimental Psychology: Animal Behavior Processes *7*, 242–268.

Sakata, J.T., and Brainard, M.S. (2008). Online Contributions of Auditory Feedback to Neural Activity in Avian Song Control Circuitry. Journal of Neuroscience *28*, 11378–11390.

Sakata, J.T., and Brainard, M.S. (2006). Real-time contributions of auditory feedback to avian vocal motor control. J. Neurosci. *26*, 9619–9628.

Schneider, D.M., Nelson, A., and Mooney, R. (2014). A synaptic and circuit basis for corollary discharge in the auditory cortex. Nature *513*, 189–194.

Schultz, W., Dylan, P., and Montague, R. (1997). A Neural Substrate of Prediction and Reward. Science *275*, 1593–1599.

Shuler, M.G., and Bear, M.F. (2006). Reward timing in the primary visual cortex. Science *311*, 1606–1609.

Skinner, B.F. (2004). "Superstition" in the Pigeon. Journal of Experimental Psychology: Animal Behavior Processes *38*, 473–479.

Soares, S., Atallah, B.V., and Paton, J.J. (2016). Midbrain dopamine neurons control judgment of time. Science *354*, 1273–1277.

Stetson, C., Cui, X., Montague, P.R., and Eagleman, D.M. (2006). Motor-sensory recalibration leads to an illusory reversal of action and sensation. Neuron *51*, 651–659.

Stetson, C., Fiesta, M.P., and Eagleman, D.M. (2007). Does time really slow down during a frightening event? PLoS ONE *2*, e1295.

Stringer, C., Pachitariu, M., Steinmetz, N.A., Okun, M., Bartho, P., Harris, K.D., Sahani, M., and Lesica, N.A. (2016). Inhibitory control of correlated intrinsic variability in cortical networks. eLife *5*, 91.

Tervo, D.G.R., Hwang, B.-Y., Viswanathan, S., Gaj, T., Lavzin, M., Ritola, K.D., Lindo, S., Michael, S., Kuleshova, E., Ojala, D., et al. (2016). A Designer AAV Variant Permits Efficient Retrograde Access to Projection Neurons. Neuron *92*, 372–382.

Ward, R.D., Kellendonk, C., Simpson, E.H., Lipatova, O., Drew, M.R., Fairhurst, S., Kandel, E.R., and Balsam, P.D. (2009). Impaired timing precision produced by striatal D2 receptor overexpression is mediated by cognitive and motivational deficits. Behavioral Neuroscience *123*, 720–730.

Welch, R.B., DuttonHurt, L.D., and Warren, D.H. (1986). Contributions of audition and vision to temporal rate perception. Percept Psychophys *39*, 294–300.

Wiener, M., Magaro, C.M., and Matell, M.S. (2008). Accurate timing but increased impulsivity following excitotoxic lesions of the subthalamic nucleus. Neurosci. Lett. *440*, 176–180.

Wittenbach, J.D., Bouchard, K.E., Brainard, M.S., and Jin, D.Z. (2015). An Adapting Auditory-motor Feedback Loop Can Contribute to Generating Vocal Repetition. PLoS Comput Biol *11*, e1004471–29.

Zhou, X., de Villers-Sidani, E., Panizzutti, R., and Merzenich, M.M. (2010). Successive-signal biasing for a learned sound sequence. PNAS *107*, 14839–14844.

Znamenskiy, P., and Zador, A.M. (2013). Corticostriatal neurons in auditory cortex drive decisions during auditory discrimination. Nature *497*, 482–485.